Journal of Energy Storage 131 (2025) 117492

Contents lists available at ScienceDirect

Journal of Energy Storage

journal homepage: www.elsevier.com/locate/est

Review article

A study on chemical kinetics of carbonates-based electrolytes for enhancing fire safety in lithium-ion batteries – A review

Ghulam Abbas Gohar [a,b,c], Liang An [b,*], Hafiz Muhammad Ali [c,d], Hao Zhao [a,*]

[a] College of Engineering, Peking University, Beijing 100871, China
[b] Department of Mechanical Engineering, The Hong Kong Polytechnic University, Hong Kong
[c] Mechanical Engineering Department, King Fahd University of Petroleum and Minerals, Dhahran 31261, Saudi Arabia
[d] Interdisciplinary Research Center for Sustainable Energy Systems (IRC-SES), King Fahd University of Petroleum and Minerals, Dhahran 31261, Saudi Arabia

ARTICLE INFO

Keywords:
Chemical kinetic mechanism
Carbonate-based electrolytes
Gas chromatography (GC)
Shock tube
Flow reactor
Molecular beam mass spectrometry (MBMS)

ABSTRACT

Lithium-ion batteries are widely used in electronics and electric vehicles for their high energy storage and long lifespan. Electrolytes are a major source of lithium-ion transportation between electrodes. However, the organic components of electrolytes can also present a fire hazard. Therefore, it is essential to investigate the oxidation of electrolytes under different oxidizing environments and analyze the chemical stability of solvents, salts, and cathode materials. To understand the reactive chemistry and fire propensity of lithium-ion battery carbonate solvents, several gas phase experimental techniques such as shock tube (ST), flow reactor (FR), jet stirrer reactor (JSR), and rapid compression machine (RCM) have been used to analyze the reaction chemistry of carbonate mixtures. Flammable gases are generated during the oxidation and pyrolysis of carbonate mixtures, and the product species can be analyzed by using MBMS and GC–MS. This review describes the chemical kinetics model of various carbonate-based electrolytes under oxidation and pyrolysis conditions, providing insights from a fire safety perspective. It is recommended to employ fundamental combustion experiments for the analysis of the decomposition and oxidation processes of carbonate-based electrolytes (DEC, DMC, EMC, EC, etc.) under low-temperature and atmospheric-pressure conditions relevant to the environment of lithium-ion batteries. This review emphasizes the recent developments in carbonate base electrolyte's chemistry, thermal stability, and their implications for fire safety.

Symbols

Equivalence ratio (Φ)
Temperature (T)
Pressure (P)
Mole fraction (X)

1. Introduction

Lithium-ion batteries (LIBs) are widely used in consumer gadgets and electric vehicles (EVs). The pursuit of safe, high-capacity, and affordable batteries has led to the prominence of lithium-ion batteries (LIBs) due to their high energy density and low cost, and subsequent concern is satisfying the demand for batteries. Annual electric vehicle battery demand is projected to reach approximately 5.5 TWh by 2030 in the Net Zero Emissions Scenario, an increase from 0.8 TWh in 2023. Nevertheless, the battery industry appears adequately equipped to meet this rising demand, as recent announcements and advancements suggest a strong capability to increase production and innovate technology [1,2]. The global demand for affordable and reliable lithium-ion batteries (LIBs) with high capacity is unprecedented. However, ongoing efforts to improve cathodes and anodes to increase capacity are hindered by safety

Abbreviations: A, Arrhenius constant; DMC, Dimethyl carbonates; EMC, Ethyl methyl carbonate; FEC, Fluoroethylene carbonate; GC–MS, Gas Chromatography and mass spectrometry; LIBs, Lithium-ion batteries; MFR, Micro Flow reactor; PFR, Plug flow reactor; ROP, Rate of production; VC, Vinylene carbonate; LBV, laminar burning velocity; FREs, Flame-retardant electrolytes; TBP, tributyl phosphate; ΔH_{vap}, heat of vaporization; CM, Compression machines; DEC, Diethyl carbonate; EC, Ethylene carbonate; Ea, Activation energy; GC, Gas Chromatography; JSR, Jet stirrer reactor; MBMS, Molecular beam mass spectrometry; PC, Propylene carbonate; SEI, Solid electrolyte interphase; R, Reaction number; DFT, Density functional theory; TEP, triethyl phosphate; ΔH_c, Lower heating value; $\Delta_c H_{liq}$, Enthalpy of combustion of liquid.

* Corresponding authors.
E-mail addresses: liang.an@polyu.edu.hk (L. An), h.zhao@pku.edu.cn (H. Zhao).

https://doi.org/10.1016/j.est.2025.117492
Received 13 February 2025; Received in revised form 27 May 2025; Accepted 16 June 2025
Available online 27 June 2025

concerns, which limit widespread adoption [3,4]. Enhancing safety is a crucial aspect of improving lithium-ion batteries, particularly due to their growing demand in electric vehicles [5,6]. Batteries failure is generally caused due to temperature, heat and chemical process. Thermal runaway can occur if the battery's temperature exceeds a threshold (usually between 130 °C to 250 °C), which is influenced by cell design, size, and electrode materials [7–11]. As the demand for electronic devices grows, higher energy density in LIBs could lead to more incidents of thermal runaway, resulting in the release of flammable gases [12–16]. Many researchers have described thermal runaway events in lithium-ion batteries as being triggers by excessive heat and temperature. As heat increases, electrolytes are consumed, which fuels a fire and eventual explosion [17–23]. To prevent battery failure, many researchers are working on lithium anodes to avoid dendrites formation and enhance lithium mobility between electrodes [24–27]. The concentration of salts in electrolytes may affect charge transfer and ohmic resistance. Moreover, a reduction in cyclic capacity of LIBs is observed when large amount of electrolyte is present [28]. The use of various additives may not only increase the viscosity of the electrolyte medium but also influence the overall volume of the electrolyte [15]. A minimum electrolyte volume factor of 3.1 times of the total volume of cell components (cathode, anode, and separator) is required for enhanced cycle stability [29]. The liquid-phase oxidation between electrolyte solutions and oxygen was investigated using Synchrotron vacuum ultraviolet photoionization mass spectrometry (SVUV-PIMS). In a closed autoclave, diethyl carbonate (DEC) was reacted with air (1 bar) and pure O_2 (10 bar) at temperature below 120 °C that suggests that it may happen early on in the thermal runaway of Li-ion batteries [30]. Characterization using synchrotron X-ray diffraction and transmission electron microscopy during in-situ heating demonstrated that the intense exothermic process is triggered by the released oxygen species. Thermal runaway is attributed to oxygen species (O_2, O^{2-}, O^-, etc.) released from cathode. The electrolyte significantly influences the thermally driven release of these oxygen species. It reduces thermal stability of cathode, potentially facilitating phase transition and oxygen release [31]. New analytical techniques have been described for examining the oxygen loss, along with potential strategies for mitigating it and the related electrochemical degradation [32]. Fig. 1 explains the thermal runway mechanism for lithium-ion batteries. Thermal runaway occurs when operating temperatures exceed the limits of 180 °C during charging and discharging cycles.

A non-flammable electrolyte prevents thermal runaway during the initial stage of failure. To improve safety, solid-state electrolytes offer a non-flammable alternative. Nevertheless, these advancements face the several challenges, including lower ionic conductivity relative to liquids, unstable solid electrolyte interface (SEI) layers, and several other difficulties associated with solid-state systems [33,34]. Flame-retardant electrolytes (FREs), specifically triethyl phosphate (TEP) and tributyl phosphate (TBP), provide a liquid alternative [35,36]. Previous studies suggested employing a high concentration of lithium salt [37–39], however this increases viscosity and reduces ionic conductivity, making it difficult to maintain battery performance. Li-ion conducting glass ceramic was employed as a solid electrolyte to prevent solid/liquid electrolyte interphase side reactions. It is desirable to employ solid electrolytes with a wider potential window, such as $Li_{6.5}La_3Zr_{1.5}Ta_{0.5}O_{12}$, and suppress side reactions and lower interfacial resistance for quasi-solid-state LIBs [40].

In the field of combustion kinetics, kinetic models of different electrolytes such as DMC, DEC, DMC/EC and EMC have been developed at high temperature and pressure. For DMC based electrolyte, the ignition delay time of DMC has been investigated in shock tube at $T = 830–1330$ °C, pressure up to 1 MPa and different equivalence ratio. DMC molecules consumed due to H abstraction at high temperature and validated with proposed kinetic model of opposed flow diffusion flame [41]. Using tunable laser absorption under high temperature (990 °C to 1390 °C), near 1 atmospheric pressure and measure time histories of CO and H_2O [42] In flow reactor, the kinetic model is validated and shows 257 species and 1563 reactions [43]. The presence of oxygen at central carbon in DMC can lead to formation of methoxy radicals, as well as low level of acetylene, ethylene, methane and ethane [44]. The methane and hydrogen gases were generated at $T = 726$ °C and along with rapid production of CO and CO_2, completing the reaction [45]. To understand the reaction mechanism of DMC, it was observed that higher burning velocity approaches the saturation point under initial conditions, with a maximum explosion pressure of 0.94 MPa [46]. The results demonstrate that DMC has a low soot formation tendency compared to other oxygenates and can contribute to NO reduction under specific fuel-rich conditions [47].

In case of rapid compression machines, the ignition delay time of dimethyl carbonate (DMC) was calculated over a temperature range of

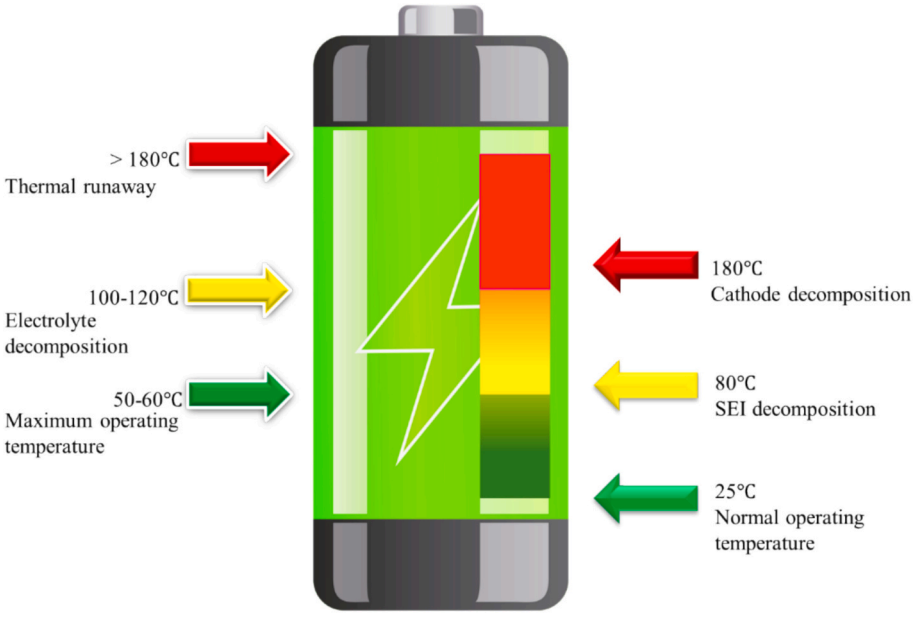

Fig. 1. General overview of temperature limits and degradation of components of lithium-ion batteries [17–21].

520 °C to 1312 °C, and at pressure up to 4 MPa. It was concluded that the reactivity of DMC is mainly due to reaction $H + O_2 \leftrightharpoons \ddot{O} + OH$, especially at low pressure and lower equivalence ratio (i.e., increasing O_2 concentration), which increases the rate of this chain reaction [48]. Under the experimental temperature range of 500–900 °C, hydrogen abstraction from DMC by CH_3O_2 (R_{2728}), HO_2 (R_{2727}), and OH (R_{2725}) enhances the system's reactivity and the unimolecular breakdown process (R_{2737}) that generate CH_3 radicals also exert a promoting influence under fuel rich conditions [49]. For diethyl carbonate (DEC) based electrolytes, in jet-stirred reactor (JSR) studies, the oxidation of DEC occurred over a temperature range of 375–825 °C, at pressure 0.1 MPa with residence of 0.07 s. At 405 °C, the concentration of DEC is decreased and early generation of carbon dioxide, ethylene, formaldehyde and ethanol [50]. At temperature $T = 505$ °C, the ethylene, CO_2 and ethanol species are measured [51]. The oxidation of DMC, DEC, and EMC was performed at $T = 325$–825 °C and 1 atm. The reactivity of carbonates ester during oxidation was found as follow the order: DEC ~ EMC < DMC, based on consumption rate. This reaction sequence was accompanied by formation of gaseous product species such as CO, CO_2, H_2, CH_4, C_2H_5OH, CH_3CHO and C_2H_4 [52].

In the case of a flow reactor, Major pyrolysis products such as C_2H_5OH, CO_2, C_2H_4 and CH_3CHO are generated during pyrolysis of DEC at temperature $T = 525$ °C [53]. The mole fraction of C_2H_4 and CO_2 increased at temperature range of 475 °C during oxidation of DEC at 1 atm [45]. Moreover, the oxidation of DEC is occurs within the range of temperature range of 275–475 °C and 1 atm [54]. In shock tube experiments, the ignition delay times, CO time histories, and laminar flame speeds for DEC combustion were measured at near-atmospheric pressure for $\phi = 0.5$, 1.0, and 2.0, over temperature of 908–1132 °C. CO profiles were recorded using Laser absorption diagnostics with a second shock tube [55].

The pyrolysis of DMC/EC has been investigated at temperature range of $T = 726$ °C where species such as CH_3CHO, CO_2, CH_2O, C_2H_4 and H_2 species were observed [56]. Various species such as C_3H_6, C_2H_4, C_2H_5OH and CO_2 are detected during the pyrolysis of DEC over the temperature range of 390–930 °C, showing good agreement with model [57]. In shock tube experiments, both DEC and EMC produced an alcohol (ethanol in the case of DEC) and (methanol in the case of EMC) which then react to yield CO at pressures (1 atm) and temperatures between 960 and 2100 °C [58].

For an EMC based electrolyte, in case of rapid compression machine, the oxidation of Ethyl methyl carbonate occurs over wide range of temperature (540–705 °C), equivalence ratio (0.5, 1, 1.5) and pressure (2–4 MPa). The H-abstraction reaction of EMC with HO_2, OH, H, and CH_3O_2 radicals produces the intermediate product such as H_2O_2, this intermediate enhances the system reactivity through chain branching, leading to generation of a significant number of OH radicals [59]. In case of constant volume combustion bomb, a new kinetic model of ethylene carbonate was developed under temperature of 250 °C and pressure (0.2 MPa), based on the basis laminar burning velocity (LBV) to better understand combustion of lithium ion batteries electrolytes [60–62]. Furthermore, the combustion characteristics of EMC/EC/DMC mixture were investigated. Increasing the EMC percentage from 25.00 % to 50.00 % results in an increase of 75.34 kW/m^2 in heat release rate, a 12.50 % escalation in flame height, and a 203.40 °C elevation in flame temperature. A higher DMC % reduces the flash point and increases the mass loss rate during combustion [63]. The combustion and chemical kinetics of different electrolytes can be investigated using various reactors and equipped with equipment such as GC and molecular beam and mass spectrometry (MBMS) as shown in Fig. 2.

In case of lithium-ion batteries cells, gas evolution occurs as a result of solvent decomposition at cathode materials. Flammable gases like hydrogen and ethylene can initiate thermal runaway, posing safety risks. Additionally, gas evolution affects cell performance, causing electrode degradation, reduced shelf life, shortened cycles, electrolyte loss, and increased cell impedance [68]. A theoretical framework has been proposed to explain how liberated lattice oxygen interacts with ethylene carbonate, leading to the formation of carbon dioxide (CO_2), carbon monoxide (CO), and water [69]. The electrolytic solvents used in LIBs consist of flammable carbonate esters [70–74]. The combustion properties of these esters were analyzed [75]. A comprehensive understanding of the reactivity and chemical reactivity of these esters is essential for improving the fire safety of LIBs. They observed the production of CO_2, H_2, and C_2H_4, which provides direct evidence of solvent oxidation reactions. Therefore, the possible pathways that can lead to LIBs fires are as follows: (1) low-temperature the decomposition of carbonate-based electrolyte generates flammable gases; (2) combustion of lithium in anode materials initiating the fire; (3) oxidation of electrolyte solvents with O_2 gas initiating the fire; (4) interaction between carbonate-based electrolytes and other forms of oxygen, such as singlet oxygen, O_2 and surface oxygen from cathode materials. However, the literature shows that electrolyte solvents do not undergoes the reaction with O_2 below 380–400 °C K without catalytical sensitization [51].

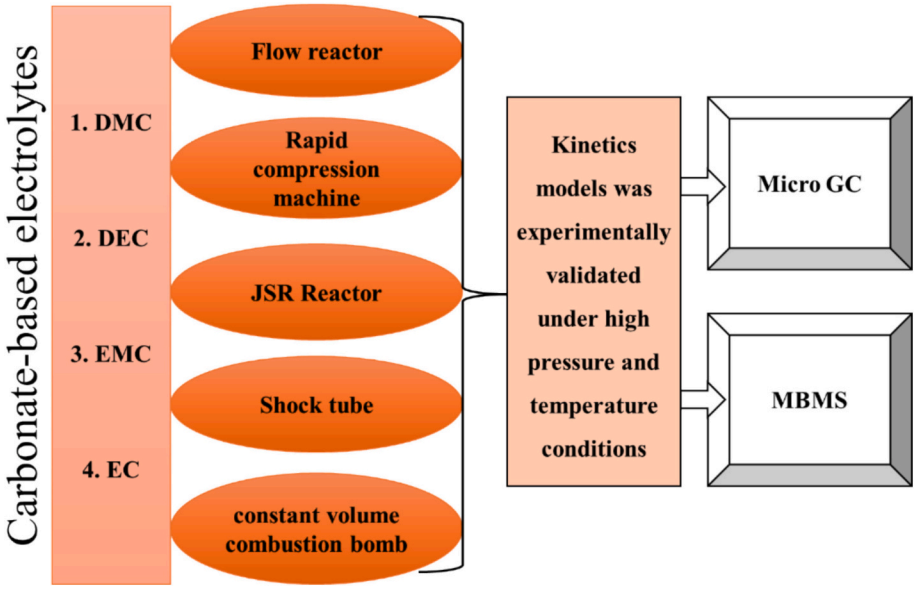

Fig. 2. Different approaches are used for chemical analysis under various conditions [43,54,57–60,64–67].

Additionally, the decomposition temperatures of DMC and DEC are even higher. Furthermore, studies [45,76] have reported a minimum ignition temperature of lithium at 630 °C in pure oxygen. Therefore, it is necessary to evaluate pathways (1–4) that may explain the failure of LIBs between the temperature limits of 125 to 200 °C, while the low-temperature oxidation of carbonate-based electrolytes occurs in various reactors. Secondly, it is crucial to investigate the reaction behavior between cathode materials and carbonate-based electrolytes using different reactors at low temperature and pressure (0.1 MPa) to better understand LIBs fires. Unfortunately, the understanding of the kinetics of their low-temperature oxidation and ignition through pathway (1–4) remains very complex and unclear due to their multi-phase interaction.

Thermal instability and fire propensity of high nickel and low cobalt (NCM) of LIBs represent one of largest challenges for commercial applications. Improving thermal stability is crucial for advanced LIBs and requires a focus on understanding interface reactions and kinetics, along with the development of advanced cathode materials. Furthermore, Investigating the low-temperature decomposition and ignition of carbonate-based electrolytes, particularly in interaction with cathode materials, remains a significant challenge. This is not only due to heterogeneous reaction pathways at low temperatures but also because of the difficulties in in-situ gas-phase and surface diagnostics. Thermal runaway in lithium-ion batteries involves both electrochemical and chemical reactions. Our focus is on the chemical aspect, particularly oxidation of electrolytes, using experiment platforms such as Shock Tube, Flow Reactor and Rapid Compression Machine. These tools provide valuable insight into fundamental chemical kinetics from ambient to combustion conditions. These methodologies provide a mechanistic understanding of the chemical behavior of electrolyte components, which is crucial for formulating comprehensive kinetic models and improving battery safety via predictive simulations. However, heterogeneous experiments involving cathode material are not yet available for these facilities. Therefore, we recommend that oxidation of these electrolytes in the presence of cathode materials be carried out in a flow reactor under controlled temperature and pressure 1 atm to simulate battery thermal runaway events. The gaseous product was analyzed by Gas Chromatography. The morphology and oxidation state of each atom of NCM were examined using SEM, EDS and XPS spectrum. We believe this combined approach is more helpful to analyze real battery failure materials. This critical review study aims to enhance the fire safety of lithium-ion batteries by investigating chemical reactions involving carbonates-based electrolytes. It utilizes various experimental setups, including flow reactors, jet-stirrer reactors, rapid compression machines, constant volume combustion bomb, and shock tubes, to examine the gas-phase decomposition of carbonate-based electrolytes under different oxidation and pyrolysis conditions. A kinetic model of carbonate-based electrolytes (DEC, DMC, EMC, EC and FEC etc.) in the literature is validated through experimental validation to analyze similar species as LIBs thermal runaways.

2. Organic carbonates-based electrolytes for lithium-ion batteries

Carbonate esters are significant components of renewable energy technologies such as lithium-ion batteries (LIBs) electrolytes. Detailed knowledge of the combustion analysis and reaction mechanism of carbonate-based electrolytes is necessary to understand the fire safety of LIBs. The number of accidents involving fires and explosions in LIBs-enabled products such as mobile phones and electric cars has risen. Common electrolyte solvents such as DMC, DEC, EC, and EMC in LIBs are considered major fire hazards [77,78]. The experiments and simulations have been conducted to identify the thermal runaway events that cause the failure of batteries and to examine the safety concerns of LIBs [79–81]. Once combustion occurs in a LIB cell, most of the heat is generated by the electrolytes [82]. The combustion enthalpy of the electrolyte is primarily determined by its solvent mixtures, regardless of the salt added [83,84]. Combustion enthalpy and vaporization enthalpy should be considered when selecting solvent mixtures in situations where flammability is a concern [75]. Most researchers are studying electrolyte flammability using auto-ignition temperature and flash point [85]. While the evaporation of liquid solvents [70,71] is the primary determinant of these features, more research into the combustion behavior or chemistry of different organic carbonates [75] is required for a better comprehension of the electrolytic combustion process. The investigation of combustion behavior remains infrequent and may lead to an inadequate assessment of the thermal safety of the electrolytes. Some studies on the combustion properties of electrolytes have been conducted. Eshetu et al. [84] used a fire propagation apparatus to study the combustion of eight typical electrolytes and found that the solvent mixture affected the enthalpy of combustion, and the lithium salt affected the hazardous byproducts. Harris et al. [75] reported significant variations in combustion and evaporation enthalpies of carbonate-based solvents during burning. Zhang et al. [86] compared the heat release rate (HRR) and mass loss rate of EC/DMC/DEC mixtures using an ISO 5660 cone calorimeter. The HRR of the oxygen consumption method and the stoichiometric method were found to be similar. Huang Qiurui et al. [87] investigated the combustion characteristics of flame retardant compounds in electrolytes under low pressure. These electrolytes play an essential role in any battery or other electrochemical energy storage device [88,89]. Fig. 3 illustrates the classification of linear and cyclic organic carbonate-based electrolytes utilized in lithium-ion batteries.

2.1. Linear carbonates-based electrolytes for lithium-ion batteries

Dimethyl carbonate (DMC), diethyl carbonate (DEC), and ethyl methyl carbonate (EMC) are linear carbonate-based electrolytes that exhibit excellent electrolyte properties for use in lithium-ion batteries, as shown in Table 1.

2.2. Cyclic carbonates-based electrolytes for lithium-ion batteries

Lithium-ion batteries can employ cyclic carbonate-based electrolytes as their electrolyte. The physical characteristics of these carbonates are explained in Table 2.

3. Oxidation and pyrolysis of carbonate-based electrolytes

Electrolytes consist of a flammable blend of cyclic and linear carbonates that facilitate the flow of lithium ion between the anode and cathode in a battery system during charging and discharging. Due to design flaws, manufacturing errors, or physical damage to the electrolyte, LIBs have been implicated in several fire events involving mobile

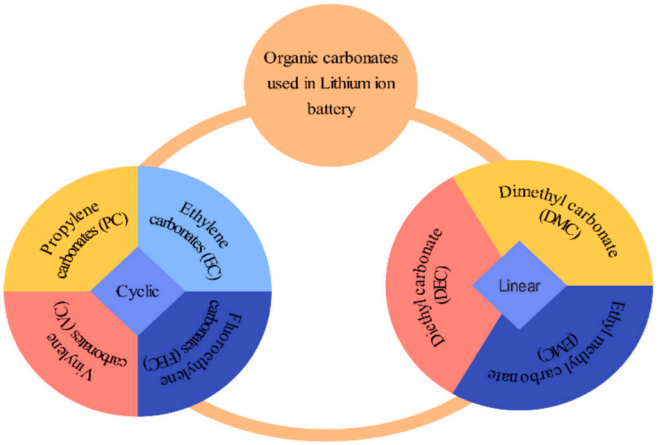

Fig. 3. Classification of organic carbonate-based electrolytes.

Table 1
Properties and structure of linear carbonates for lithium-ion batteries.

Sr #	Linear carbonate	Properties	Structure
1	Dimethyl carbonate (DMC) [90]	Formula: $C_3H_6O_3$ Density: 1.069 g/cm^3 Boiling point: 91 °C Flash point: 18 °C ΔH_c (MJkg^{-1}): 14.48 ΔH_{vap} (MJkg^{-1}): 0.43 $\Delta_c H_{liq}$ (MJkg^{-1}): −15.78	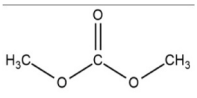
2	Diethyl carbonate (DEC) [78]	Formula: $C_5H_{10}O_3$ Density: 0.975 g/cm^3 Boiling point: 126 °C Flash point: 57 °C ΔH_c (MJkg^{-1}): 22.7 ΔH_{vap} (MJkg^{-1}): 0.34 $\Delta_c H_{liq}$ (MJkg^{-1}): −22.7	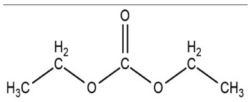
3	Ethyl methyl carbonate (EMC) [90]	Formula: $C_4H_8O_3$ Density: 1.01 g/cm^3 Boiling point: 110 °C Flash point: 23 °C ΔH_c (MJkg^{-1}): 22 ΔH_{vap} (MJkg^{-1}): 0.34 $\Delta_c H_{liq}$ (MJkg^{-1}): −22	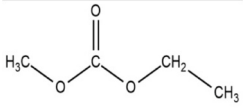

Table 2
Properties and structure of cyclic carbonates for lithium-ion batteries.

Sr #	Cyclic carbonate	Properties	Structure
1	Propylene carbonate (PC) [78]	Formula: $C_4H_6O_3$ Density: 1.2 g/cm^3 Boiling point: 242 °C Flash point: 145 °C ΔH_c (MJkg^{-1}): −27.4 ΔH_{vap} (MJkg^{-1}): 0.55 $\Delta_c H_{liq}$ (MJkg^{-1}): −27.4	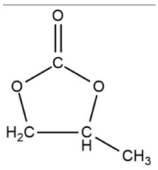
2	Ethylene carbonate (EC) [90]	Formula: $C_3H_4O_3$ Density: 1.3210 g/cm^3 Boiling point: 248 °C Flash point: 146 °C ΔH_c (MJkg^{-1}): 12.66 ΔH_{vap} (MJkg^{-1}): 0.62 $\Delta_c H_{liq}$ (MJkg^{-1}): −13.29	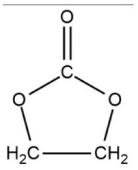
3	Fluoroethylene carbonate (FEC)	Formula: $C_3H_3FO_3$ Density: 1.41 g/cm^3 Boiling point: 249.5 °C Flash point: 101.7 °C $\Delta_c H_{liq}$ (MJkg^{-1}): −10.4	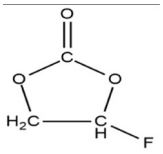
4	Vinylene carbonate (VC)	Formula: $C_3H_2O_3$ Density: 1.35 g/cm^3 Boiling point: 162 °C Flash point: 72.7 °C $\Delta_c H_{liq}$ (MJkg^{-1}): −13.29	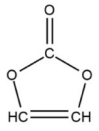

phones to airplanes [73,91,92]. With rapid increase in the number of electric vehicles on the roads [93], which utilized large scale LIBs, it has become essential to understand the mechanical damage that may occur under real world conditions. Additionally, analyzing the combustion and chemistry of the reaction between the LIBs electrolyte components is necessary for developing strategies to reduce their flammability [75,94]. The oxidation and kinetics of diethyl carbonate [45,51,53,54,66,95–99], the pyrolysis and oxidation of dimethyl carbonate (DMC) [41–43,48,75,99–102], the oxidation and kinetics of ethyl methyl carbonate [45,76,98] and reaction kinetics of ethylene carbonate [60] were investigated.

3.1. Thermal decomposition characteristic of dimethyl carbonates (DMC)

(a) Pyrolysis and oxidation of dimethyl carbonate (DMC)

Dimethyl carbonate, a crucial carbonate-based solvent used in lithium-ion battery electrolytes [103,104], undergoes oxidation and pyrolysis under diverse conditions of temperature and pressure in various combustion mode such as shock tube, flow reactor and rapid compression machines [41–43,45,46,48,105]. This study aims to investigate its behavior across various temperature and pressure ranges. Its reactivity is remarkable, with pressure and equivalence ratio significantly impacting ignition delay, particularly at low and high pressures conditions [48]. The experiments and kinetics analysis in a shock tube provide valuable insights into its decomposition mechanisms which are driven by H-abstraction reactions, notably the primary chain branching reaction:

$$\dot{H} + O_2 = \ddot{O} + OH \quad (1)$$

Sensitivity analysis highlights the significance of this reaction across various temperature ranges [41].Moreover, the mixture of DMC/O_2/He/Ar was experimentally studied in a shock tube under varying conditions [42]. Due to the absence of C—C bonds, dimethyl carbonate (DMC) produces lower amounts of ethylene and acetylene. The O-C-O bonds in DMC can be cleaved due to oxygen on the main carbon atom. As a result, a methoxy radical and small amounts of CH_4, C_2H_4, and acetylene are produced [44]. The high-temperature pyrolysis of DMC yielded a wide array of intermediates and products which results the a comprehensive kinetic model consisting the 257 species and 1563 reactions [43]. The DMC/air model slightly overpredicted some burning velocities but provided accurate prediction of for flame temperature power exponent (α) [105]. For detailed reaction mechanism of DMC under various combustion techniques, are explained in Table 3.

It is concluded that the oxidation of DMC, a carbonate-based electrolyte occurs within the temperature range of $T_{w,max}$ = 725–875 °C, while the mole fractions of H_2, CO, CH_4, C_2H_4, and C_2H_6 increase within narrower range of $T_{w,max}$ = 776–826 °C. Alexandrino et al. [48] corrected the DMC thermal decomposition rate constant (Eq. (2)) from the Sun to Hu mechanism.

$$DMC = CH_3OCO + CH_3O \quad (2)$$

Under oxidizing conditions, the consumption of DMC involves radical H-atom abstractions. Various mechanisms have been proposed

Table 3
Summary of reaction mechanisms of various DMC models at different temperatures and pressure [41–43,45,46,48,105].

Sr. No	Mixture	Temperature (°C)	Φ	Pressure (MPa)	Combustion method	Ref.
1	DMC/O_2/Ar	T_5 = 826–1326	0.5–2.0	P_5 = 0.12, 0.5, 1	Shock tube (ST)	[41]
2	DMC/O_2/Ar	T_f = 1970, 2045	1.0, 1.5	0.0027, 0.0033	Burner stabilized premixed flame	[43]
3	8%DMC/N_2, 39%O_2/N_2	T_f = 1352	Non-premixed	0.1	Opposed flow diffusion flame	[44]
4	DMC/O_2/Ar(/He)	T_5 = 1033–1368	0.5–2.0	P_5 = 0.125–0.133	Shock tube	[42]
5	2%DMC/Ar	568–1216	∞	0.004, 0.020, 0.1	Plug-flow reactor	[43]
6	DMC/O_2/(N_2 or Ar)	Tc (T_5) = 521–1311	0.5–2.0	Pc (P_5) = 0.2, 2, 4	Rapid compression machine, shock tube	[48]
7	1.5%DMC/O_2/N_2	426–1026	1.0	0.1	Micro flow reactor	[45]
8	1.5%DMC/N_2	426–1026	∞	0.1	Micro flow reactor	[45]

by Glaude et al. [100] analogies to alkanes, Hu et al. [41] to methyl butanoate [106], and Sun et al. [43] to methyl formate [107]. The reactions with O and H radicals were calculated using theoretical rate constants [64,65]. Thermal degradation rate constants differ between the Hu and Sun mechanisms.

$$DMC = CH_3OCH_3 + CO_2 \quad (3)$$

CO_2 elimination rate constants from the Glaude and Sun mechanisms were respectively applied in the Hu and Sun mechanisms. Fig. 4 demonstrates the product species, observed during oxidation and pyrolysis of DMC and compares the results simulation models with experiment data [45].

(b) Reaction pathway of dimethyl carbonate (DMC)

Alexandrino et al. [48] proposed a DMC kinetic model that describes the ignition delay time of the oxidation mechanism and breakdown of DMC. The chemical reaction pathway conducted at 20 % DMC conversion reveals that the predominant pathways for DMC consumption involve two unimolecular breakdown processes of DMC and the abstraction of H-atoms from DMC, mostly by Ḣ atoms and ȮH radicals. Reaction pathways of DMC with different concentrations (1.75 and 0.75 %) $T = 1076$ °C, $\varphi = 1.0$ and pressure $P = 2$ atm is illustrated in Fig. 5.

Fig. 6 describes sensitivity analysis of DMC oxidation. The most significant reactions increasing reactivity are the chain-branching reaction $\dot{H} + O_2 \rightleftarrows \ddot{O} + \dot{O}H$ (R_8) and the fuel-specific reaction R_1 [48].

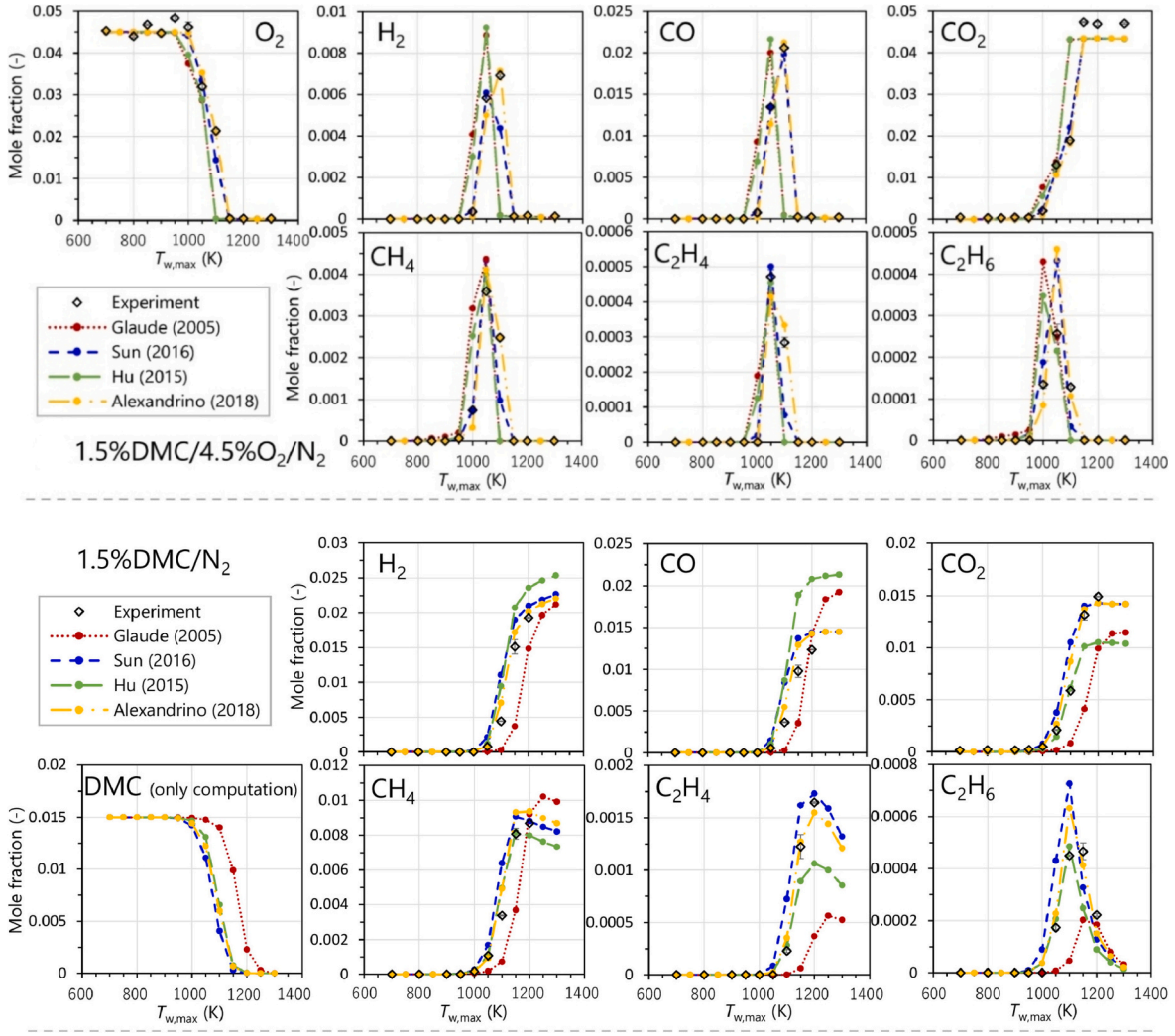

Fig. 4. The concentration of different species were measured (the open diamond) and calculated (the circle with a line) of DMC mixtures [45].

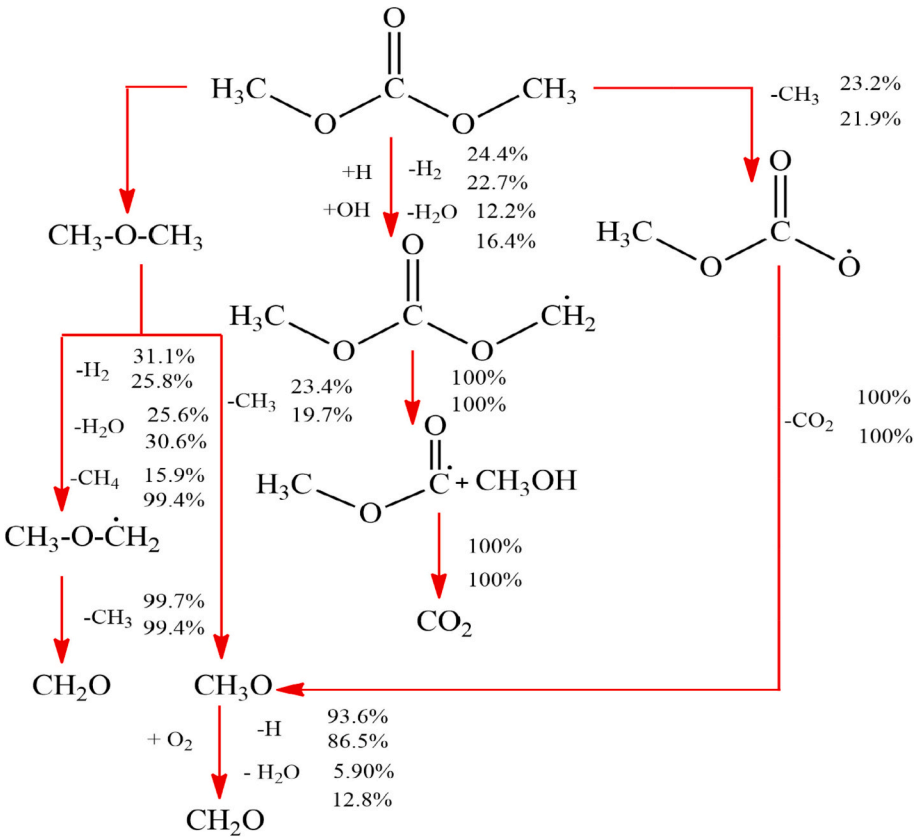

Fig. 5. Reaction pathways of DMC with different concentration (1.75 and 0.75 %) $T = 1076$ °C, $\varphi = 1.0$ and pressure P = 2 atm [48].

Increasing fuel concentration makes the specific fuel reaction more sensitive, but the chain-branching reaction less sensitive.

K. Alexandrino [108] proposed the DMC kinetic model at high pressure (20, 40, and 60 atm), different temperature (500–1073 K) and describe the reaction pathway of DMC using model's reaction rate analysis as shown in Fig. 7. Throughout all the stoichiometries and pressures examined in this study, the predominant consumption of DMC occurs through reactions with CH_3O_2 and OH radicals. This reaction is facilitated by increased oxygen concentration under fuel-lean conditions, leading to subsequent breakdown of DMC and formation of methyl radicals and CO_2.

W. Sun et al. [43] used Chemkin Pro to investigate the premixed flames, flame speeds, ignition delay time and opposed-flow diffusion flames for the DMC Kinetic model. The disintegration of the $CH_3OC(=O)OCH_2$ radical also produces a significant quantity of CH_3OCO radical, more than 90 % of which decomposes into CO_2 and CH_3. Furthermore, the $CH_3OC(=O)O$ radicals generated from the direct bond cleavage of the fuel are entirely transformed into CO_2 and CH_3O radicals. Furthermore, the molecular removal of CO_2 from DMC facilitates the production of CO_2. The three fuel-related processes, along with the reaction $CO + OH \rightleftharpoons CO_2 + H$, account for nearly all CO_2 production as shown in Fig. 8.

Fig. 9(a & b) illustrates the principal reaction pathways of DMC/air mixtures at points where 30 % of each fuel is burned at temperature $T_w = 760$ °C, along with similar pathways at the same temperature $T_w = 560$ °C for comparative analysis. While fuel consumption reactions are minimal at low temperatures $T_w = 560$ °C, CO generation via the C_1 pathway accelerates swiftly following the consumption of DMC at $T_w = 760$ °C. According to the analysis of DMC oxidation reactions, The key difference between their reactivity and that of C_2H_4 producing thermal decomposition reactions is the fuel consumption activities that occur during H-atom abstraction events in DMC [45].

K. Kanayama et al. [56] described the EC/DMC pyrolysis reaction pathways with 30 % reactant consumption. EC is mostly used by R_1, which creates CO_2 and acetaldehyde. The chemical route of EC that produces CO_2 and ethylene oxide (C_2H_4O) (R_2) was the second most energetically preferred decomposition reaction based on theoretical calculations; however, it had little effect on EC pyrolysis under the examined conditions. CO_2 elimination produces DME (CH_3OCH_3) (R_4) the main DMC consumption process. The CH_3–O bond dissociation channel is the second lowest channel energetically. The current reaction pathway consumes 30 % DMC at $T_w = 867$ °C, and this dissociation channel contributes 18 %. According to the reaction path study, EC mostly decomposes into stable species (CO_2 and acetaldehyde) and has little effect on DMC consumption. After EC and DMC unimolecular breakdown, all reaction paths reach CH_3, CO, and CO_2. CH_3 then recombines to form the C_2 species, which evolves progressively, as shown in Fig. 10.

3.2. Thermal decomposition characteristic of diethyl carbonates (DEC)

(a) Pyrolysis and oxidation of diethyl carbonate (DEC)

Diethyl carbonate (DEC) is common electrolyte in lithium ion batteries [44]. DEC oxidation and combustion was examined in different combustion approaches such as shock tube, flow reactor, rapid compression machines and jet stirrer reactor [45,50,51,53,54]. Oxidation species were investigated utilizing a jet stirrer reactor operating at 10 atm and temperatures ranging from 225 °C to 925 °C, along with equivalence ratios of 0.5 to 2.0. A chemical kinetic model was constructed for DEC and validated using experimental data, enabling the prediction of changes in concentrations of intermediate species and ignition times. The agreement between the model and experimental results was assessed for evaluation [51]. This study explored DEC's higher temperature oxidation and pyrolysis. Initially, the [-OC(=O)O-]

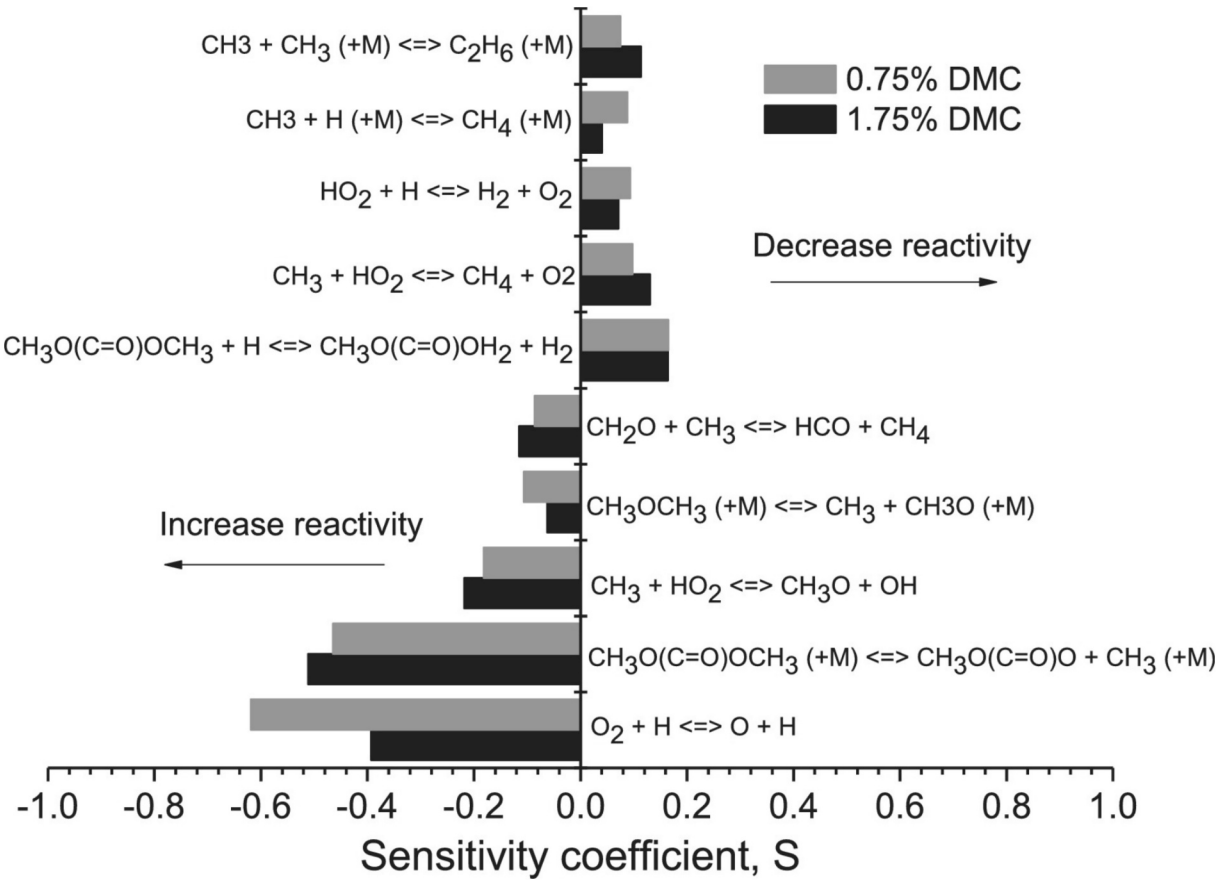

Fig. 6. Sensitivity analysis at $P = 2.0$ atm, and T = 1076 °C for 0.75 % DMC & 1.75 % DMC [48].

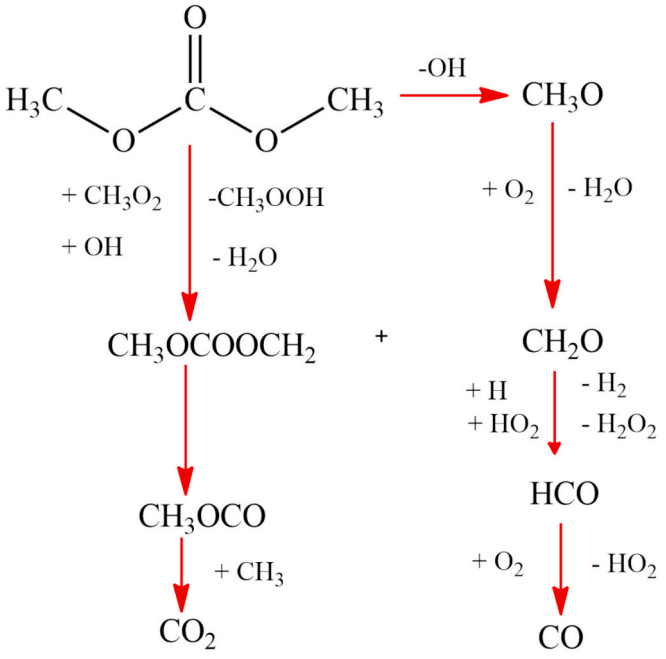

Fig. 7. Reaction pathway of DMC oxidation under high pressure [108].

group in DEC enhances CO_2 production during premix flame conditions, breaking down $C_2H_5OC(=O)OH$ and leading to the generation of intermediates such as C_2H_4, CH_3CHO, C_2H_5OH, and C_2H_5 through β-scissions of radicals like $C_2H_5O\dot{C}(=O)$ and $C_2H_5OC(=O)O^{\bullet}$ [53]. The oxidation of DEC initiates CO_2 generation at low temperatures ($T_{w,max}$ = 475 °C) because of its ester/carbonate group. Oxidation generates C_2H_4 and C_2H_5OH even at low temperatures [45]. Oxidation initiates at 375 °C with DEC and at 175 °C with O_3, indicating its low-temperature characteristics. A DEC/O_3 kinetic model was developed, demonstrating considerable accuracy, but with a minor overestimation in the range of 275–475 °C. The DEC oxidation trajectory with O_3 demonstrates accurate predictions within the range of 275–475 °C. The O_3 promotes DEC oxidation by generating active O atoms that do not engage in direct reactions with DEC [54].The reaction mechanism of DEC is explained in Table 4.

Fig. 11(a) illustrates that the mole fraction of O_2 observed during DEC oxidation decreases steadily from $T_{w,max}$ = 626 °C (900 K) to near depletion at $T_{w,max}$ = 776–826 °C (1050-1100 K). At $T_{w,max}$ = 626 °C (900 K), mole fractions of H_2, CO, CH_4, and C_2H_6 peak at 676–726 °C (950–1000 K). The CO_2 and C_2H_4, key species in DEC combustion, increase at lower temperatures ($T_{w,max}$ = 476 °C (750 K)), whereas oxygen declines slightly. Between $T_{w,max}$ = 576 °C and 726 °C (850 & 1000 K), the CO_2 mole fraction stabilizes around 0.074 by 826 °C (1100 K). Compared to theoretical and experimental predictions, the Sun mechanism and Nakamura technique estimate O_2, H_2, CO, CH_4, and C_2H_6 mole percentages properly. The two methods forecast CO_2 and C_2H_4 mole fractions differently at low temperatures ($T_{w,max}$ = 476–576 °C (750–850 K). The pyrolysis of DEC is shown in Fig. 11(b), above 726 °C (1000 K), both the Nakamura and Sun methods align, showing similar trends for increasing H_2, CO, and CH_4 fractions. However, the DEC, CO_2,

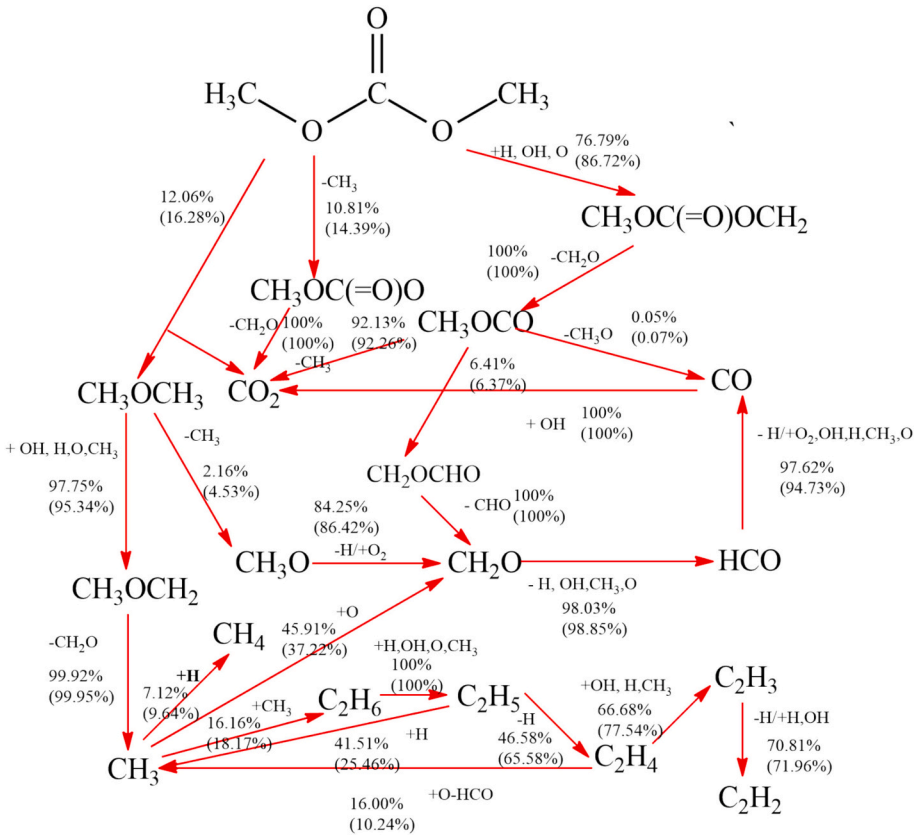

Fig. 8. Analyses of DMC reaction routes at different $\varphi = 0.1$ and 1.5 using ROP [43].

C_2H_4, and C_2H_5OH fractions differ between the methods.

Fig. 12(a) and (b) depict concentration of DEC and O_2 at different temperatures with varying levels of O_3 addition. The experimental findings show that, in the absence of O_3 addition, DEC oxidation commences at 376 °C (650 K), and low-temperature reactivity is not observed, which aligns with prior literature [51]. Conversely, when O_3 is added, the oxidation of DEC occurs at a significantly low temperature from 176 °C (450 K), which intensifies with higher O_3 concentrations. The present study of DEC/O_3 model predicts low temperature DEC oxidation well in the presence of O_3. however, it slightly overestimates DEC and O_2 consumption at 276–476 °C (550–750 K), indicating uncertainties in the low-temperature DEC oxidation pathway [54].

Fig. 13(a) & (d) depict the concentration of CO, CH_3CHO, CH_2O, and CO_2 at various temperature range with addition of O_3 The evaluation of these species from 176 °C (450 K) occurs and indicates low temperature oxidation [54].

The molecules of C_2H_4 and C_2H_5OH are not produced lower than 376 °C (650 K) which are not primary products during oxidation of DEC. This implies that C_2H_4 and C_2H_5OH are not significantly affected by O_3 levels at low temperatures, as observed in the experimental and simulations results. The O_3 begins to quickly disintegrate around 176 °C (450 K) with agreement with our previous findings [54].

(b) Reaction pathway of diethyl carbonate (DEC)

Zhao, Hao, et al. [54] investigated the oxidation of diethyl carbonate (DEC) in flow reactor at various temperatures range from 126 to 576 °C (400–850 K) and with addition of O_3. They developed a kinetic model for diethyl carbonate/O_3 system, and its predictions were found to be highly accurate, except for DEC oxidation between temperature of 276–476 °C (550–750 K), where model somewhat overpredicted reactivity. Following the H-atom abstraction reaction, diethyl carbonate forms the molecule such as $C_2H_5OCOOC{\cdot}HCH_3$ through the reaction involving OH and $\dot{O}$ radicals.

The molecule of $C_2H_5OCOOC{\cdot}HCH_3$ oxidizes with O_2 to produce $C_2H_5OCOOCH(OO){\cdot}CH_3$. Two molecules, $C_2H_5OCOOC.HCH_3$ and $C_2H_5OCOOCH(OO){\cdot}CH_3/HO_2{\cdot}/CH_3O_2$, react with each other to generate $C_2H_5OCOOCH\left(\dot{O}\right)CH_3$.The molecule of $C_2H_5OCO\dot{O}$ and CH_3CHO are generated through decomposes of $C_2H_5OCOOCH\left(\dot{O}\right)CH_3$ using β-scission mechanism, and finally produces the CO and CO_2 as demonstrated in Fig. 14.

K. Kanayama et al. [45] studied the DEC/air kinetic model, which was based on the Alexandrino mechanism [41]. The reaction pathways of DEC/air mixture were investigated, where 30 % of fuel is burned at temperature at $T_w = 555$ °C and $T_w = 755$ °C, as shown in Fig. 15(a and b). The oxidation of DEC at a low temperature ($T_w = 555$ °C) produces a variety of intermediate and final products, such as C_2H_5OH, C_2H_4 and CO_2. However, these products are relatively stable, and only a small number of active radicals are formed. Although a radical loop uses up oxygen and generates hydrogen peroxide and hydroxyl radicals (HO_2) by performing two-step reactions from CH_3CHO to C_2H_5OH, the radical loop oxidation enhancement is still rather weak when carried out at low temperatures.

W. Sun et al. [53] proposed a reaction pathway for diethyl carbonate (DEC) in which the degradation of DEC happens. Although the six-membered elimination DEC⇋$C_2H_5OC(=O)OH + C_2H_4$ is responsible for limiting DEC consumption under pyrolysis and primary mechanism of DEC degradation is due to H-atom abstraction from the diethyl carbonate (DEC).

About 50 % of the DEC is decomposed by H-abstractions from secondary carbon atoms, whereas only about 22 % is used up by those from main carbon atoms (because of varying strengths of the C—H bonds involved). Two distinct fuel radicals $CH_3CHOC(=O)OC_2H_5$ and

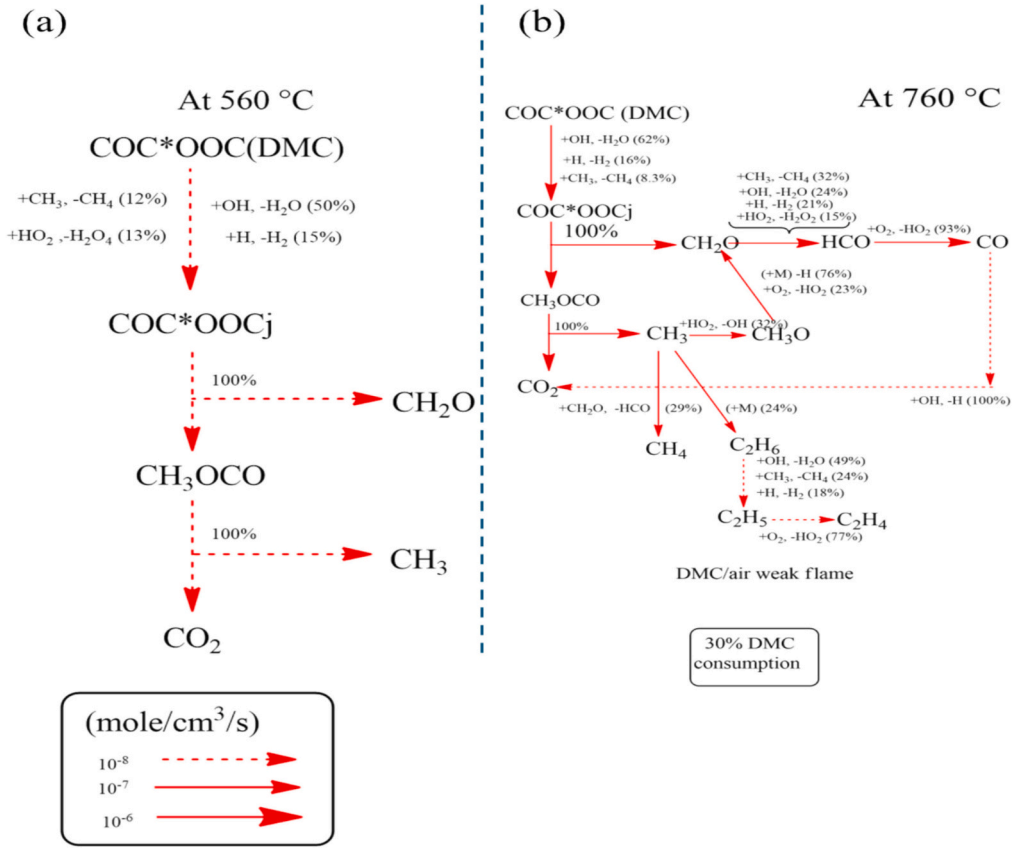

Fig. 9. Reaction paths of DMC/air weak flames [45] estimated using the Alexandrino mechanism [48].
Copyright © 2017 The Combustion Institute. Reproduced from Elsevier.

$CH_2CH_2OC(=O)OC_2H_5$, are produced, which easily degrade and generate smaller species. The three principal products seen in pyrolysis investigations (CO_2, C_2H_4, and C_2H_5OH) are present in high levels in the premixed flame, but their generation paths may differ from those reported in pyrolysis. According to the ROP study, C_2H_5OH is produced solely from the degradation of $C_2H_5OC(=O)OH$, just like in pyrolysis, whereas CO_2 and C_2H_4 are formed by several processes, as shown in Fig. 16.

H. Nakamura et al. [51] explained the oxidation of DEC at high temperature ignition and species concentration in a jet stirred reactor. Fig. 17 depicts the reaction mechanism of DEC oxidation in the JSR at 50 % fuel consumption at different conditions ($T = 506$ °C, $P = 10$ atm). Fig. 18 depicts the chemical pathway of DEC was performed at 526 °C, 30 atm.

3.3. Thermal decomposition characteristic of ethylene carbonate (EC)

(a) Oxidation and pyrolysis of ethylene carbonate (EC)

The ethylene carbonate (EC) is a widely utilized as electrolyte in LIBs due to its high dielectric constant [74,109]. Limited studies have explored the behavior of EC. The decomposition of EC radical cation suggests that the likely outcome is the generation of CO_2. Xing et al. [110] employed the DFT model (B3LYP/6-311++G(d,p) and confirming CO_2 formation. Unlike dialkyl carbonates, the unique structures of linear and cyclic carbonates lead to distinct decomposition pathways, often involving CO_2 production. Investigation into the combustion of EC is vital for comprehending the chemical events associated with LIB flames. Harris et al. [75] proposed a kinetic model to estimate energy and product release rates. Therefore, the development of a kinetic model for ethylene carbonate is crucial. K. Kanayama et al. [56] studied CO_2, CO, H_2, and C_1-C_2 hydrocarbon species using gas chromatography at different temperature conditions (T = 426–926 °C). The reaction mechanism of DMC/EC is explained in Table 5.

The EC compound experiences a rapid decrease and is completely consumed at $T = 726$–776 °C (1000–1050 K), whereas concentration of DMC begins to decrease at a higher temperature range ($T = 776$–825 °C (1050–1100 K) and is fully consumed at 926 °C (1200 K). The concentration of H_2, CH_4, and CO sharply increase at 1100 K, while CO_2 begins to rise within temperature range where EC is consumed at T = 726–776 °C (1000–1050 K). At 776 °C, C_2H_6, C_2H_4, and C_2H_2 are successively generated. DME and CH_2O increase sharply escalate between 726 and 776 °C (1050–1100 K), mirroring the decline of DMC. CH_3CHO, a reliable EC decomposition indicator, peaks at 776 °C, followed by a rapid decline. In summary, EC decomposes earlier than DMC, which aligns with the theoretical projections shown in Fig. 19.

3.4. Thermal decomposition characteristic of ethyl methyl carbonate (EMC)

(a) Pyrolysis and oxidation of ethyl methyl carbonate (EMC)

EMC, a linear carbonate, was decomposed in a microflow reactor (MFR) under various equivalence ratios, at a pressure of 1 atm and temperature (426–1026 °C). Gas chromatography identified several product species (CO, O_2, CH_4, H_2, CO_2, C_2H_2, and C_2H_4). The production of CO_2 occurred in two stages: initially during fuel degradation at 576 °C K, and subsequently through CO oxidation at 776 °C. EMC decomposition yielded CO_2 and C_2H_4, along with CH_3OH, which was formed via methyl formic acid. The oxidation of CH_3OH and C_2H_4 led to a secondary increase in CO_2 [88]. Table 6 explains the reaction mechanism and combustion method of ethyl carbonate.

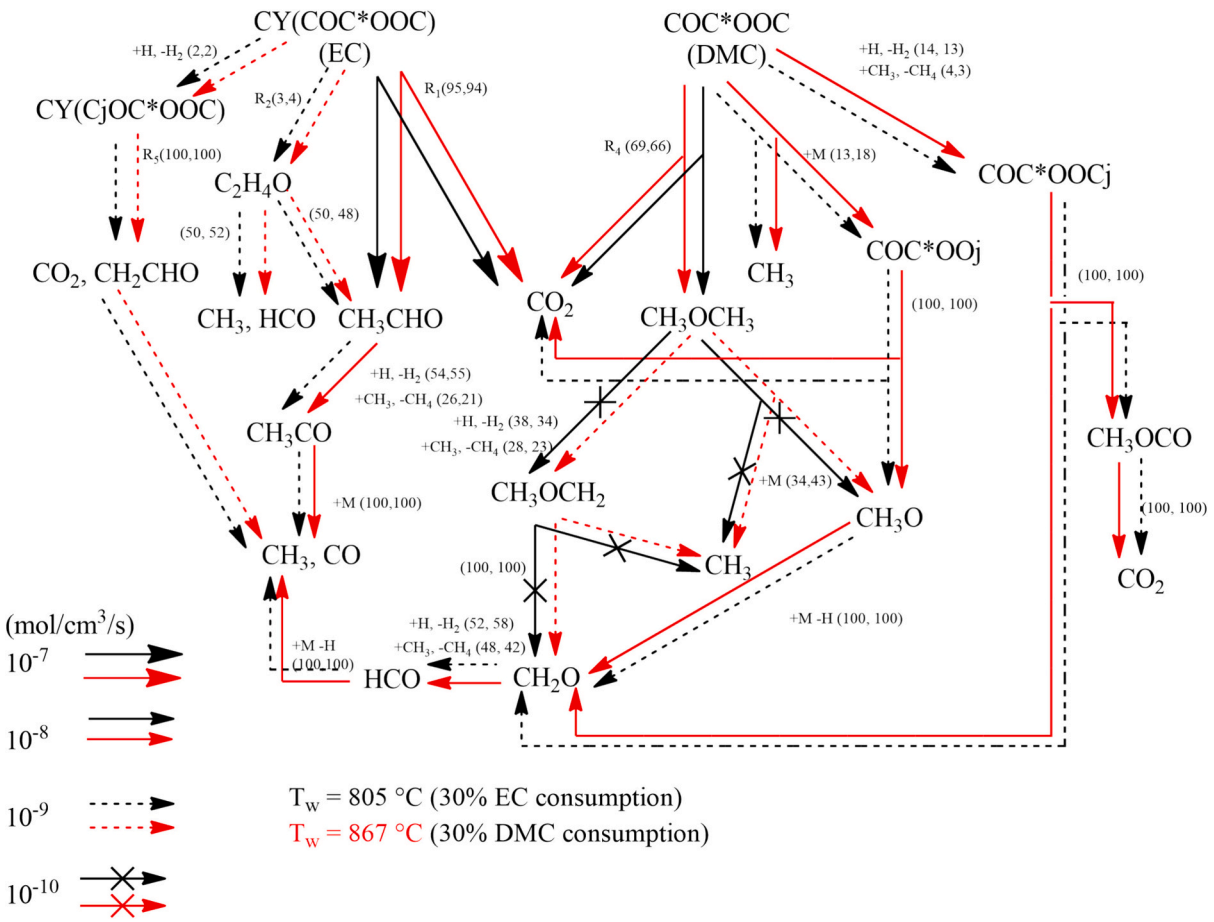

Fig. 10. Reactions pathways that occur during the pyrolysis of EC and DMC. The primary reaction routes are indicated by the black and red arrows. At $T_{w,max}$ = 926 °C, 30 % of the EC (at T_w = 756 °C) and 30 % of the DMC (at T_w = 867 °C) are consumed [56]. (For interpretation of the references to colour in this figure legend, the reader is referred to the web version of this article.)

Table 4
Reaction mechanism of different DEC models at different temperature and pressure [45,50,51,53,54].

Sr. #	Mixture	Temperature (°C)	Φ	Pressure (MPa)	Combustion method	Ref.
2	0.1%DEC/N_2/O_2	T_0 = 286–946	0.5–2.0	0.1	SP; Jet-stirred reactor	[50]
3	DEC/air	Tc (T5) = 386–1026	0.5–2.0	3	Rapid compression machine, shock tube	[51]
4	0.1%DEC/N_2/O_2	226–926	0.5–2.0	1	Jet-stirred reactor	[51]
5	DEC/O_2/50%Ar	2162	1.5	0.15	Burner stabilized premixed flame	[53]
6	1.5%DEC/N_2	426–726	∞	0.1	Micro flow reactor (MFR)	[45]
7	1.5%DEC/O_2/N_2	426–1026	1.0	0.1	Micro flow reactor (MFR)	[45]
8	0.5%DEC/O_2/Ar/He	126–576	1.2	0.1	Atmospheric laminar flow reactor	[54]
9	0.5%DEC/O_3/Ar/He	126–576	1.2	0.1	Atmospheric laminar flow reactor	[54]
10	2%DEC/Ar	418–863	∞	0.004, 0.020, 0.1	Plug-flow reactor	[53]

The findings reveal that EMC decomposition yielded C_2H_4 and CO_2 without consuming oxygen at temperatures of 476–576 °C (750–850 K). At high temperature, oxygen consumption and the generation of H_2, CO, and CH_4 commenced. The EMC reaction progressed in multiple stages: at temperature (T = 476–576 °C), different species such as C_2H_4 and CO_2 are produced, at temperature (T = 626–726 °C), the conversion of decomposition products into carbon monoxide (CO) occurs, and at 776 °C, the oxidation of CO to carbon dioxide (CO_2) takes place. Furthermore, a significant fraction of H_2 and CO observed around 626–726 °C (900–1000 K) as shown in Figs. 20 and 21(a and b) [76].

(b) Reaction pathway of ethyl methyl carbonate (EMC)

A kinetic model for ethyl methyl carbonate has been developed and validated it experimentally using flow reactor [76]. Fig. 22(a and b) illustrates the primary reaction pathway of EMC during oxidation at 576 °C and 776 °C. At 576 °C, the decomposition of EMC occurs to produce COC^*OOH and C_2H_4 through reaction of R_1, which is the main reaction, while other EMC breakdown processes (R_2 and R_3) contribute far less than R_1 does. The reaction R_4 quickly breaks down, releasing CO_2 and CH_3OH, and low temperature prevents C_2H_4 and CH_3OH from reacting with one other. However, these reactions continued at 776 and 576 °C. The methanol is oxidized to CO and CO_2 through the C_1 pathway and ethene (C_2H_4) mostly produces CH_3 radicals and C_2 species. At 776 °C, the EMC decomposition reaction was negligible when compared to the oxidation of ethene and methanol.

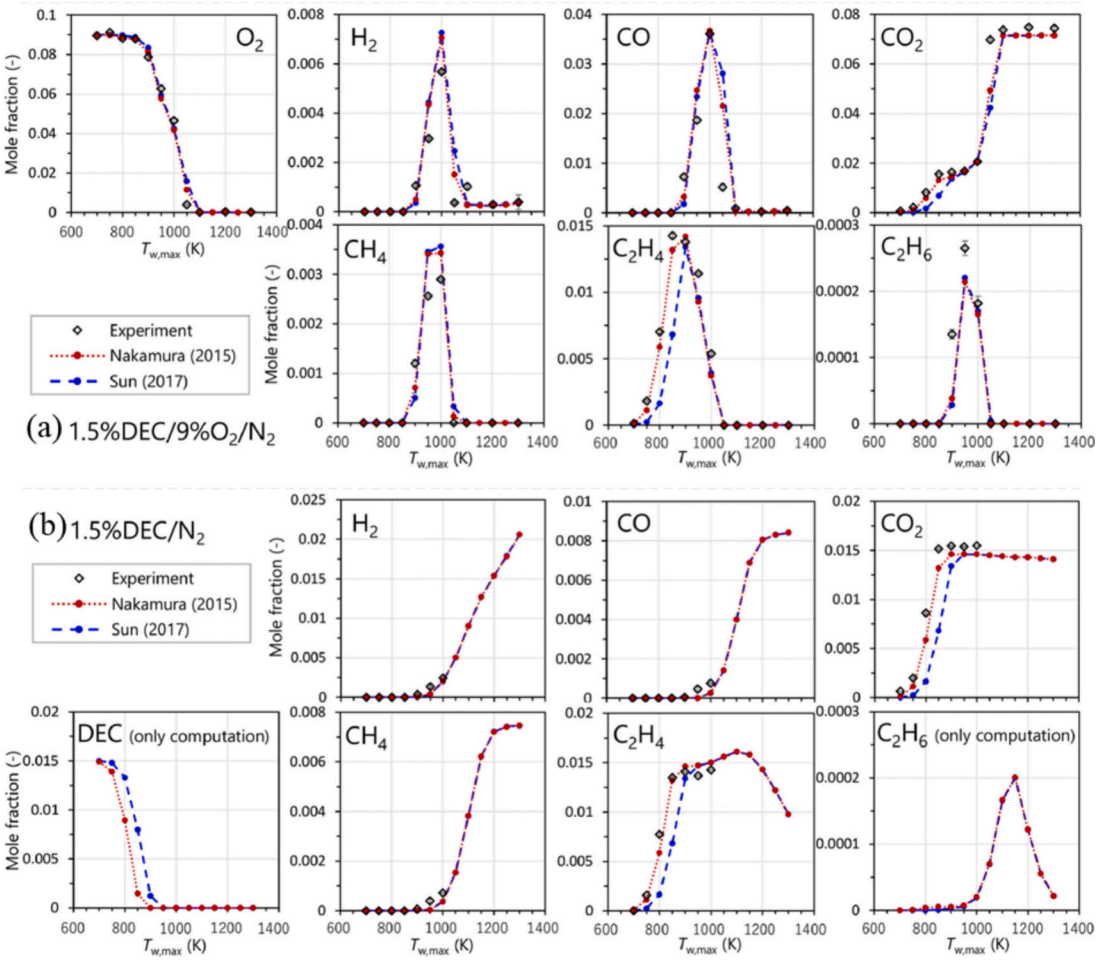

Fig. 11. The mole fractions of different species were measured (the open diamond) and calculated (the circle with a line) of DEC mixture (a) Oxidation od DEC (b) Pyrolysis of DEC [45].

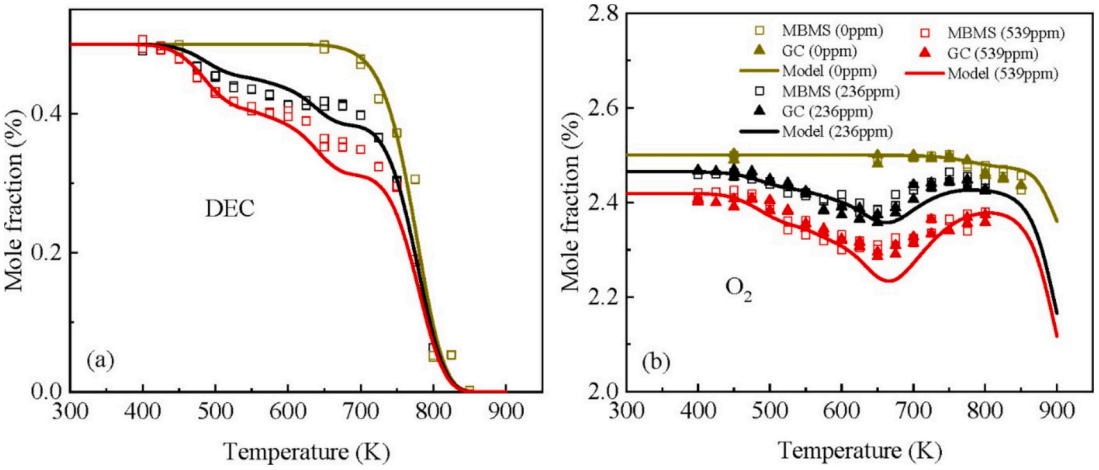

Fig. 12. Consumption of (a) DEC (b) O_2 concentration at different temperature and pressure 1 atm [54].

3.5. Thermal decomposition characteristic of propylene carbonate (PC)

(a) Degradation of propylene carbonate (PC)

A quantum chemical investigation was conducted to analyze the degradation process and kinetics of propylene carbonate (PC) in the presence of the hydroxyl radical (OH), as illustrated in Fig. 23 [111] and the resulting products from the studied reactions encompass OCHO, CH_3CHO, CH_2O, and CO_2.

Fig. 24 scheme (a) illustrates the possibility of the alkyl radical

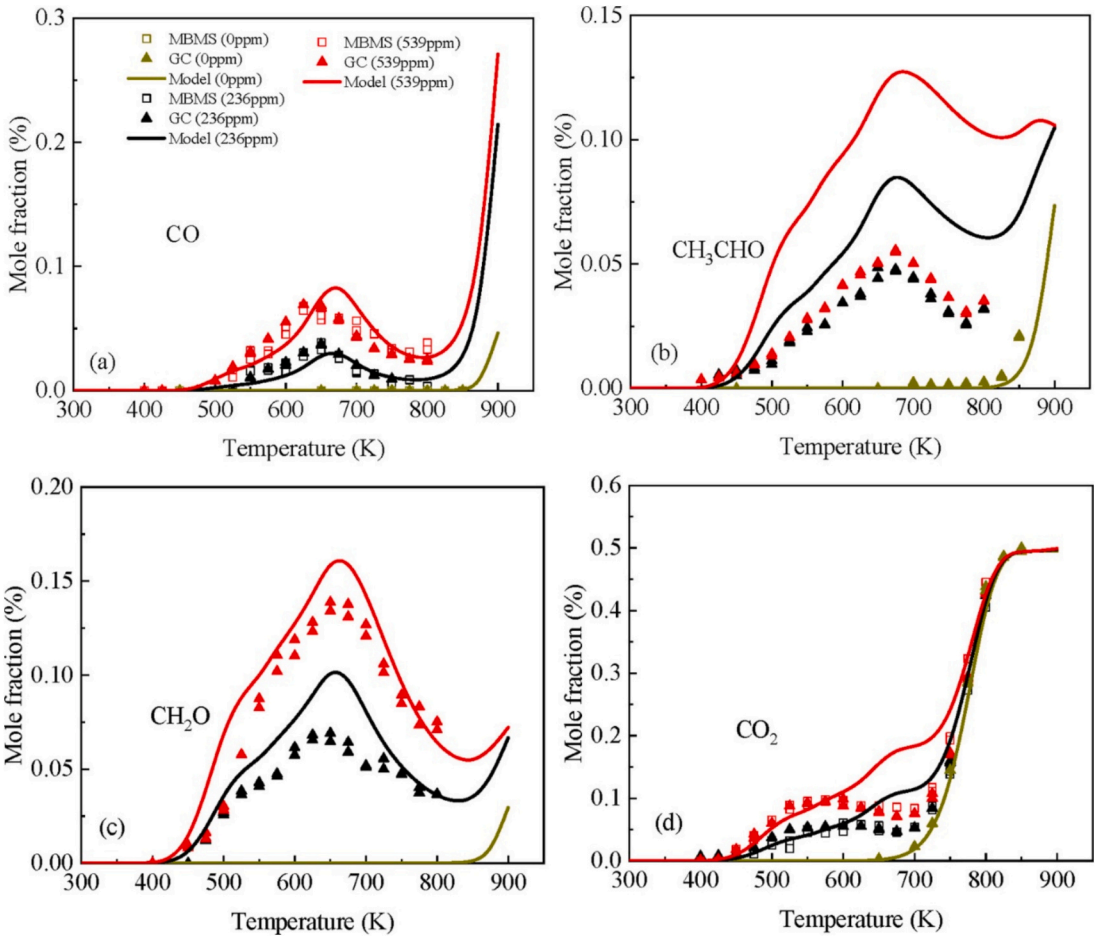

Fig. 13. Evolution of (a) CO (b) CH_3CHO (c) CH_2O (d) CO_2 at different temperature and pressure 1 atm [54].

undergoing subsequent reactions, resulting in the formation of a cyclic keto carbonate or glyoxal.

Fig. 24 in scheme (b), the removal of hydrogen atom from methyl group of propylene carbonate occurs and generates alkoxy radical which can undergo a variety of reactions. Fig. 24 scheme (c) proposes the potential elimination of a methyl group by the alkoxy radical, resulting in the formation of a keto-cyclo-carbonate. However, the absence of carbonate absorption in the product spectrum, along with the presence of formaldehyde (HCHO) and methanol (CH_3OH), indicates a different outcome. The involvement of additional methyl radicals in the generation of these compounds suggests that this reaction pathway is not significant. The primary reaction route for this radical involves the opening of its ring through the breakage of a C—C or C—O bond. Methyl glyoxal could be synthesized using the C—O bond breakage strategy, however it is not considered because it is not present in the product spectrum. C—C bond cleavage is then assumed to be the primary process, leading to the resynthesis of acetyl formyl anhydride [112].

4. Functionalized electrolyte additives for thermal and electrochemical stability

Various additives such as borates [113], phosphates [114], nitrates [115], phosphates [114], quercetin [116], polymers [117], and carbonates are used for improving safety as shown in Fig. 25. These chemicals produce a protective layer on the surface that enhances battery safety without diminishing cycle performance. Moreover, several chemicals enhance cellular thermal resistance at elevated temperatures. Transition metal ions such as Ni, Co, and Mn are commonly found in lithium-rich oxides. The transition metal ions solubilize in the carbonate-based electrolyte during the charge and discharge cycles of these oxides. Dissolution leads to structural degradation and a reduction in cathode capacity, hence diminishing battery performance [118].

5. Discussions and recommendations

Researchers have developed the kinetic model of carbonate-based electrolytes (DMC, DEC, EMC and EC) in which they concluded that most electrolytes are stable below 380 °C in gas phase reaction. The oxidation and pyrolysis of electrolytes have been conducted in flow reactors, rapid compression machines, shock tubes and plug flow reactors at high temperature, high pressure and low residence time. In actual scenarios, lithium-ion batteries can fail in temperature range of 125–225 °C. The temperature of lithium-ion batteries can increase because of lithium migration and electrochemical processes. Generally, this temperature rise has a minimal impact on the performance and safety of the batteries during regular usage. Nevertheless, in cases of battery misuse where excessive heat is generated, it can trigger internal electrochemical side reactions that produce substantial heat and flammable gases. This could potentially result in a thermal runaway incident. As the solid electrolyte interphase (SEI) degrades, the temperature of lithium-ion batteries can elevate within the range of 80 °C to 120 °C. This causes the breakdown of the meta-stable substance present in the SEI, resulting in the production of carbon dioxide (CO_2), oxygen (O_2), and flammable hydrocarbons. Oxygen (O_2), known for its strong oxidizing properties, has the potential to worsen electrochemical side reactions within lithium-ion batteries. Additionally, oxygen (O_2) acts as

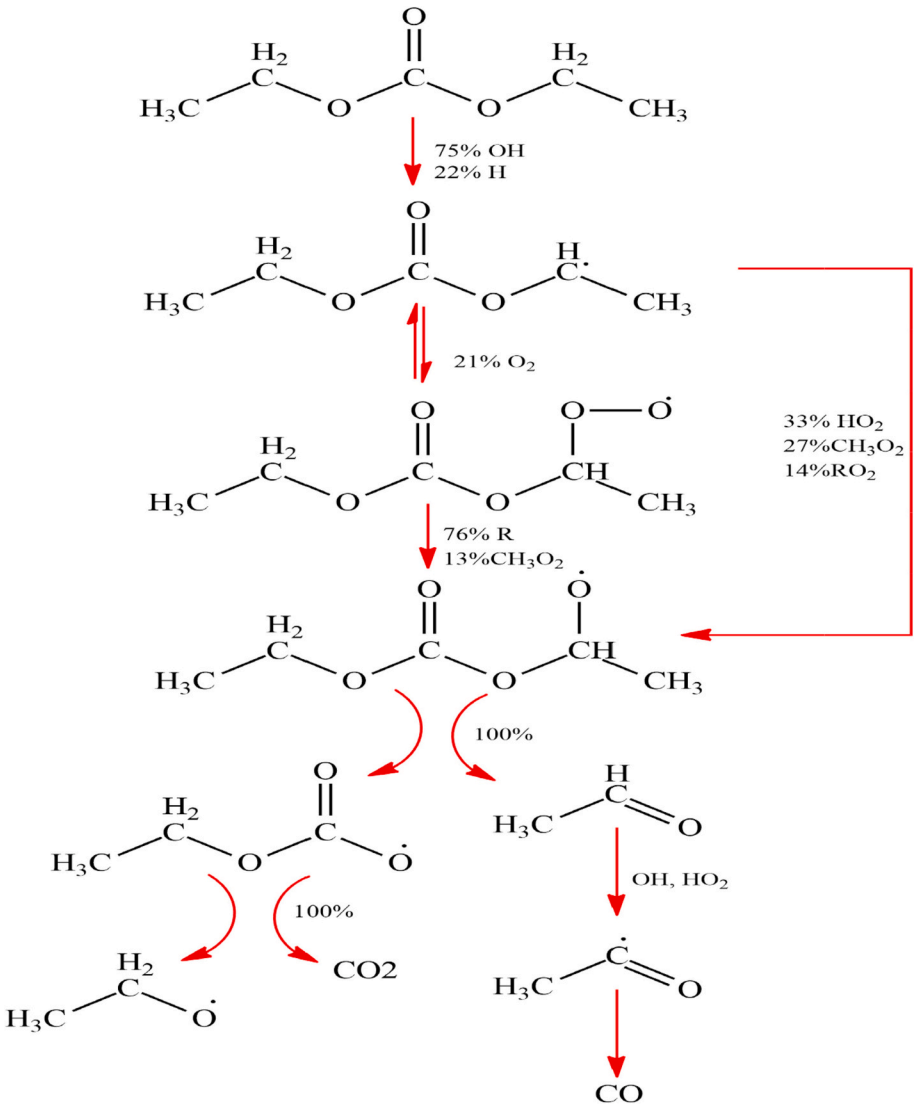

Fig. 14. Schematic of DEC at and 1 atm with 539 ppm O_3 [54].

a combustion enhancer, posing an additional safety risk. These flammable gases, produced from the interactions between electrolytes and electrodes, are commonly served as fuel for battery combustion and explosion except for CO_2 under thermal abuse conditions. Their combustion kinetics have been comprehensively studied in the combustion society [119] and not emphasized in this work. The fire safety of batteries can be highly improved by inhibiting the production of flammable gases especially for H_2 and C_2H_4, which exhibit broader flammable ranges and higher flame speeds and heat releases. Therefore, we have to understand the oxidation chemistry of electrolytes for producing these gases and emphasize their correlation with thermal runaway in this work.

On the contrary, electrolyte radicals such as H, CH_3, and C_2H_5 undergo degradation processes that have the potential to produce additional hydrocarbon gases (CH_4, C_2H_6, C_3H_6, C_3H_8, and H_2) at higher temperatures. Elevated temperatures can lead to the evaporation of the electrolyte. As exothermic reaction progresses, the reaction rate intensifies, leading to a rapid increase in internal battery pressure caused by the emission of gases. If the internal pressure exceeds a specific threshold compared to the external ambient pressure, the battery can burst and disintegrate. The decomposition of electrode materials releases gases that are expelled from the battery, resulting in the formation of a significant smoke stream. Ultimately, this can lead to fires or even explosions [120,121]. Excessive heat in the battery can source oxidation of the electrolyte and vent out of the cells. The released gases can ignite immediately or with a delay, posing a risk of a subsequent gas explosion. In heating and fire incidents, lithium-ion batteries emit various toxic compounds, including carbon monoxide and carbon dioxide [122–124]. It was concluded that thermal runway starts from temperature 150 °C by investigating the cell voltage, time and temperature profile using visualize accelerating rate calorimetry (ARC) [80]. It is possible to see how the liquid electrolyte in a battery sample fluctuates and how the protective plastic layer deforms when heated (150–200 °C) to the point of thermal runaway [125].

This review focuses on the thermal runaway problem in lithium-ion batteries where oxidation of electrolytes is carried out at low temperature and pressure. It can be investigated that thermal runaway problems can be solved by using kinetics reaction of electrolyte in different reactors. It will be a big achievement in the field of batteries where we can analysis the reaction mechanism of electrolyte with cathode materials and understand the real scenario of thermal runaway. The oxidation of electrolytes can be investigated in different reactors such as flow reactors in which we can select the different residence time, low temperature ranges 25–375 °C and 1 atm pressure and the kinetic model of

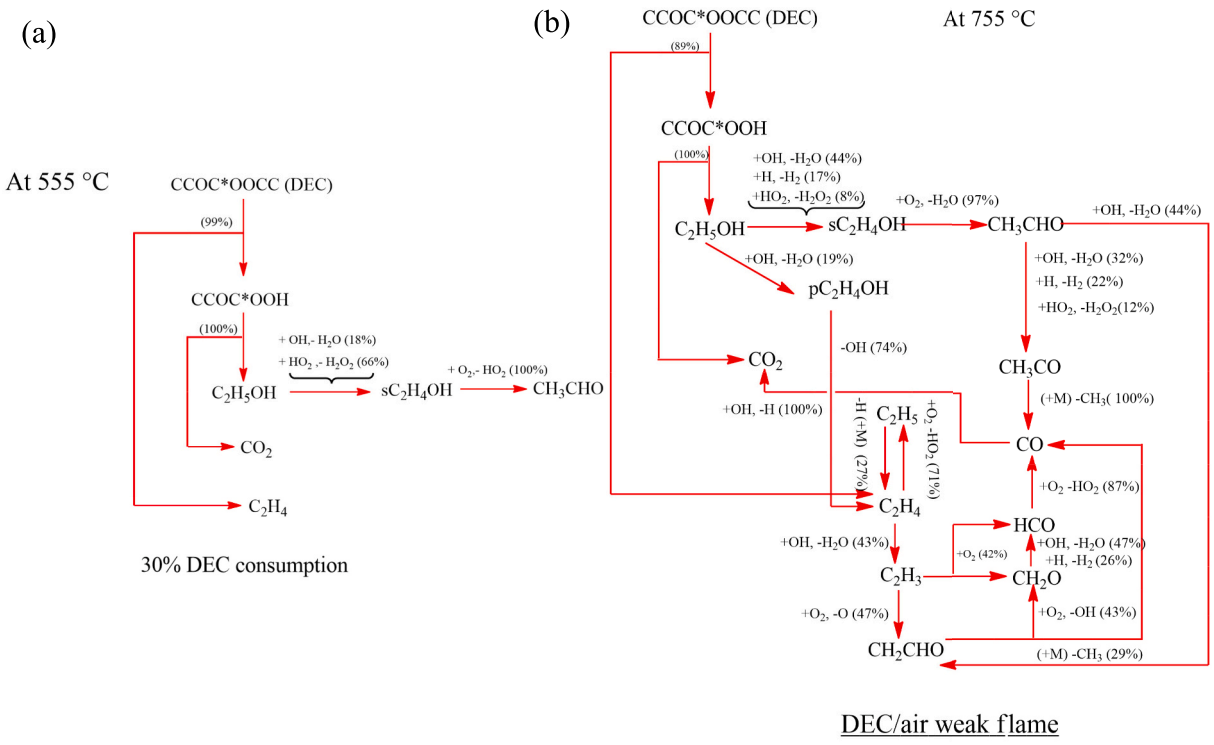

Fig. 15. Reaction paths of DEC/air weak flames [45] estimated using the Alexandrino mechanism [48].
Copyright © 2017 The Combustion Institute. Reproduced from Elsevier.

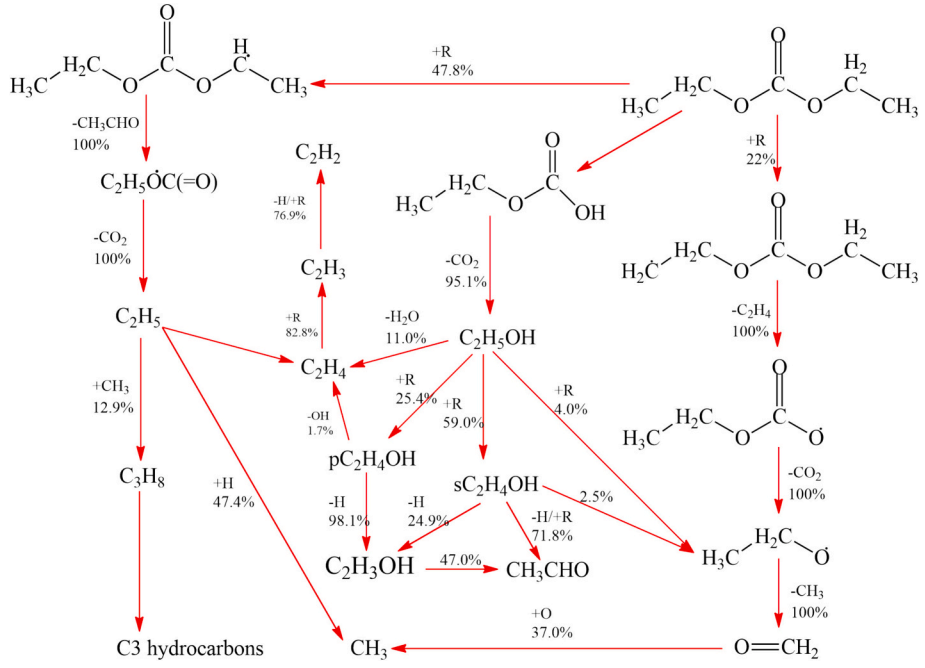

Fig. 16. Premixed flame DEC reaction pathways based on comprehensive ROP analysis [53].
Copyright © 2017 The Combustion Institute. Reproduced from Elsevier.

electrolyte can be developed at low temperatures and pressure. Secondly, it can be analyzed the interaction between electrolytes and cathode materials at long residence time, low temperature, and pressure to develop the batteries environment. Authors can provide a clear image of thermal runaway events in the field of oxidation kinetics of electrolytes to combustion society and bridge the gap between the communities of LIBs. Fig. 26(a) describes degradation of different parts of batteries at various temperature during operational conditions [17–21]. Fig. 26(b) explains the combustion kinetics of different carbonated based solvents at high temperature and pressure [43,45,53,54,56,58,66,95]. Fig. 26(c) describes future recommendations and research gaps between communities of LIBs and fundamental combustion behavior of carbonate-based electrolytes.

There are two types of reactions that happen in batteries, 1.

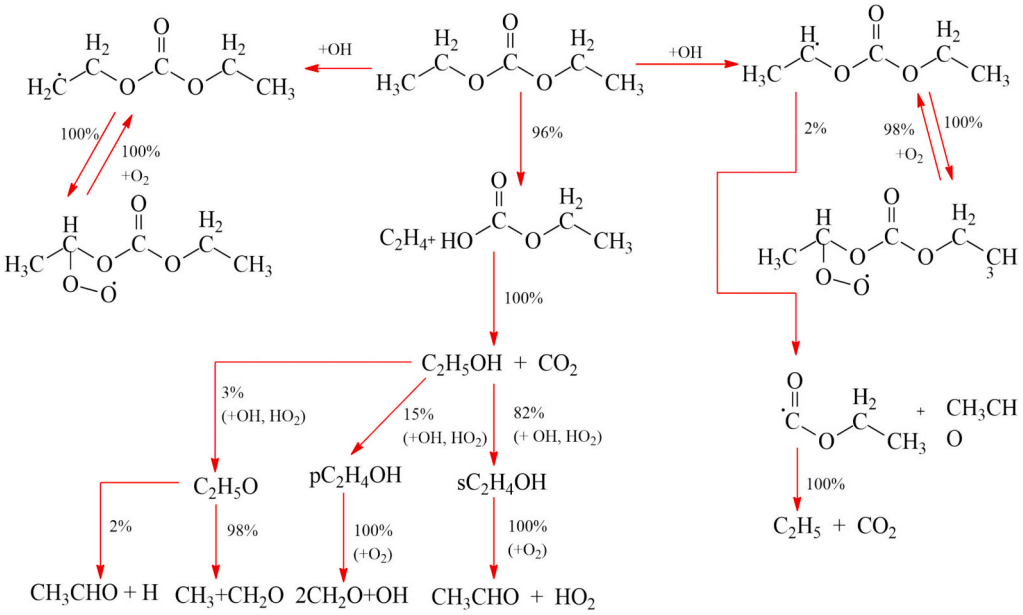

Fig. 17. Chemical reactions involving the oxidation of DEC in a JSR under 10 atm & T = 506 °C [51].

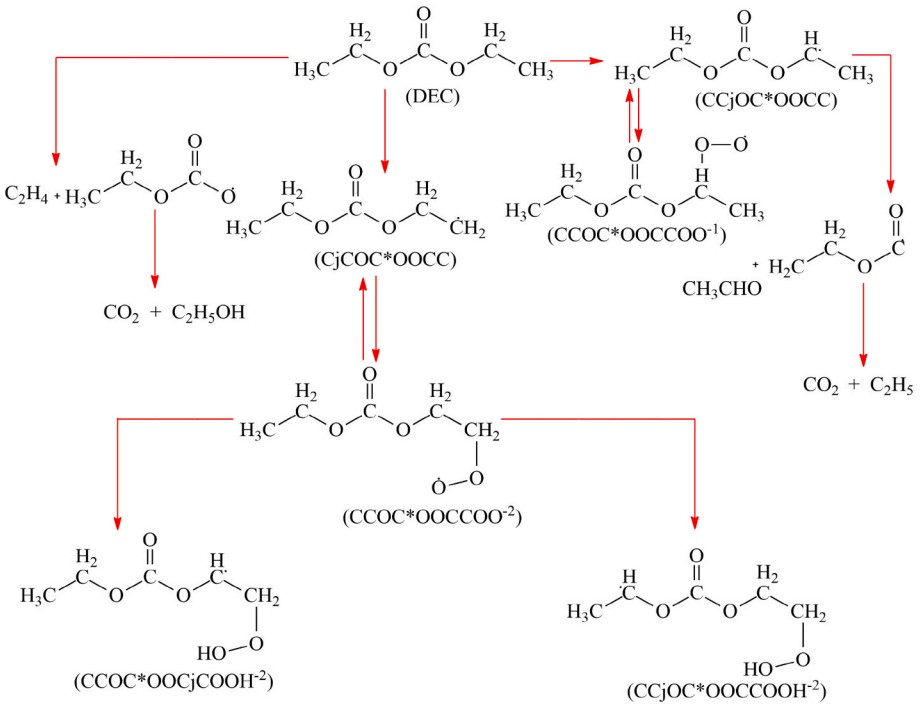

Fig. 18. Reaction pathways of Ignition of DEC at 526 °C, 30 atm [51].

Table 5
Reaction mechanism of ethyl carbonate model at different temperature and pressure [56].

Sr. #	Mixture	Temperature (°C)	Φ	Pressure (MPa)	Combustion method	Ref.
1	0.088% DMC/ 0.112%EC/ 99.8%N_2	T_0 = 426–926	–	0.1	Micro flow reactor (MFR)	[56]

Electrochemical reaction 2. Chemical reaction. A significant research gap exists under heterogeneous reaction between electrolyte and cathode, particularly to identify the thermal runaway species. We focus on chemical reactions specifically, how electrolyte oxidation happens. High temperature techniques such as shock tube, flow reactor, rapid compression machines have been used to study electrolyte oxidation. There is lack of research on low temperature and pressure oxidation of these that resemble the real operational environment of electrolyte and cathodes. We proposed a real time experimental approach for thermal stability of electrolytes and cathode. In order to simulate DEC under low

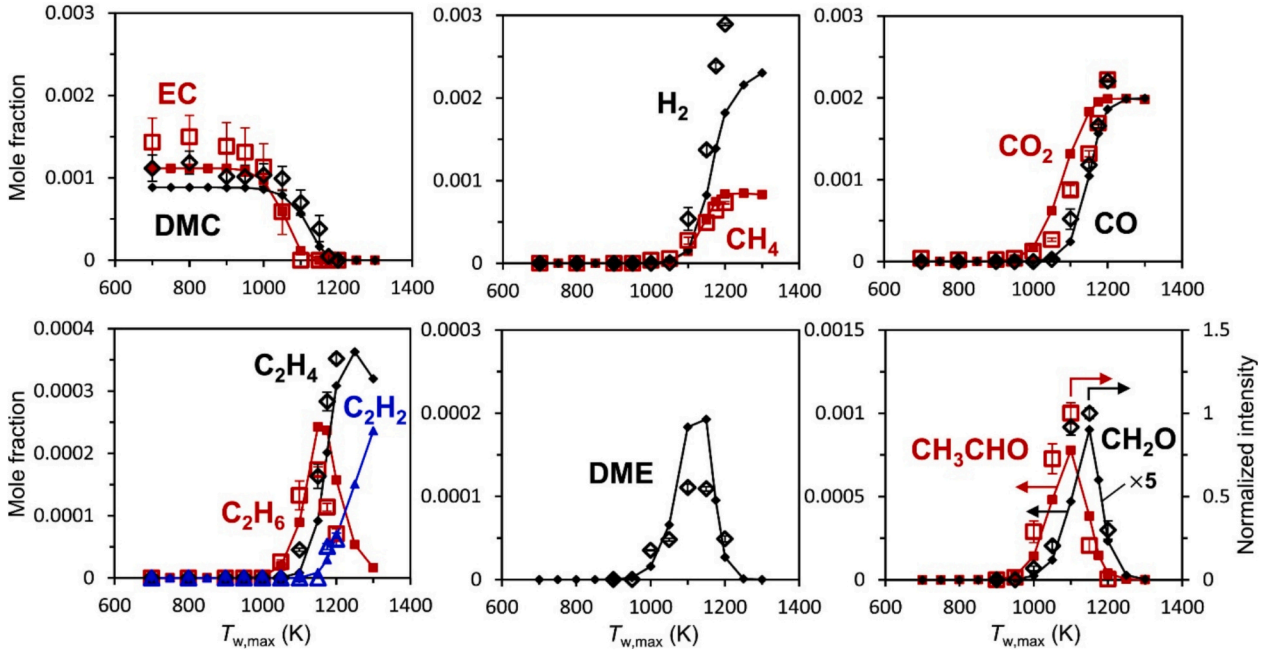

Fig. 19. The concentration (mole fraction) of DMC, EC, H_2, and C_1-C_2 species were determined both through measurement (open symbol) and computation (closed symbol with a line) [56].

Table 6
Reaction mechanism of ethyl carbonate model at different temperature and pressure [76].

Sr. #	Mixture	Temperature (°C)	Φ	Pressure (MPa)	Combustion method	Ref.
1	EMC/O_2/N_2	426–1026	∞	0.1	Micro flow reactor (MFR)	[76]

temperature and 1 atm pressure conditions that are pertinent to real battery environments, a previously developed kinetic model of DEC must be used. We propose to use a gas chromatograph (GC), coupled with a flow reactor to validate the model. NCM particles will be suspended in a flow reactor and allowed to interact with gaseous electrolytes. Chemical reactions happen for long residence time in reactors, enabling the quantification of generated species and providing real time insights into reaction dynamics. Furthermore, low temperature thermal runaway species is important in critical safety concern, as it often

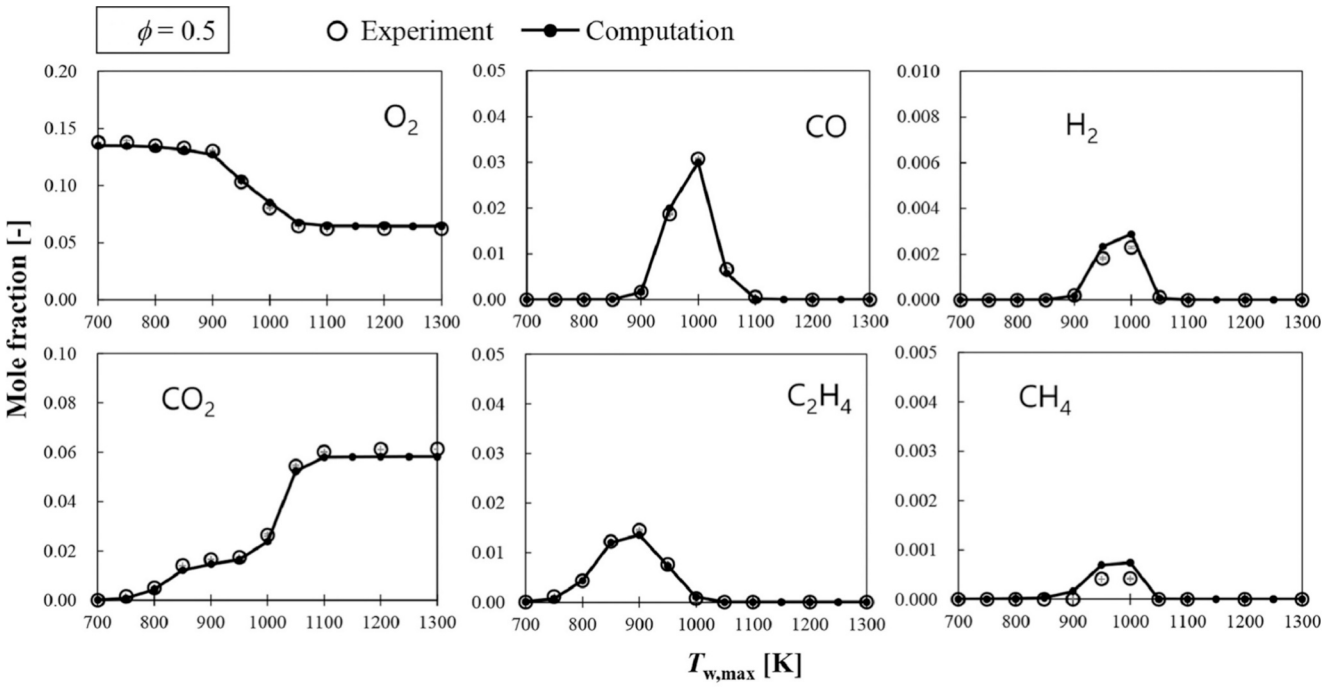

Fig. 20. The oxidation of EMC in MFR was determined at atmospheric pressure with a mixture of 1.5%EMC/O_2/N_2 with different equivalence ratios [76].

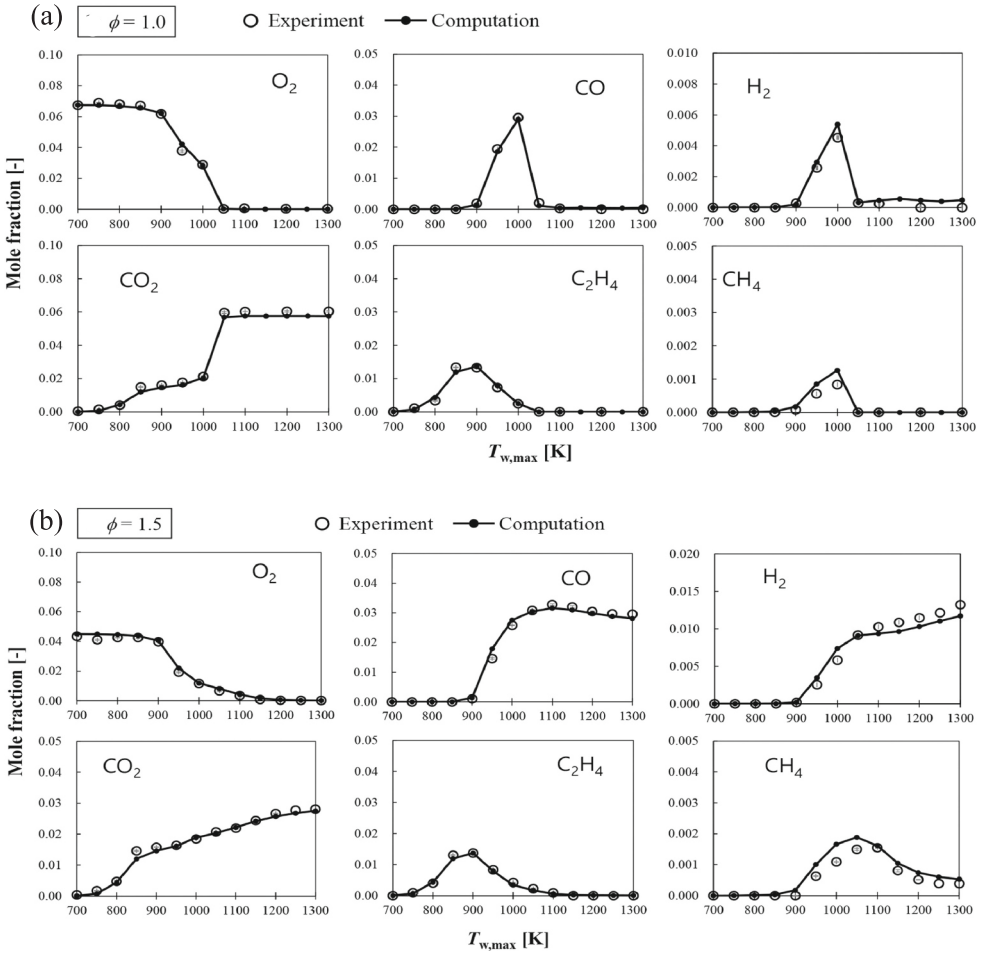

Fig. 21. (a and b). The oxidation of EMC in MFR were determined experimentally (using symbols) and through computer simulations (using lines) at atmospheric pressure with a mixture of 1.5%EMC/O_2/N_2 with different equivalence ratios [76].

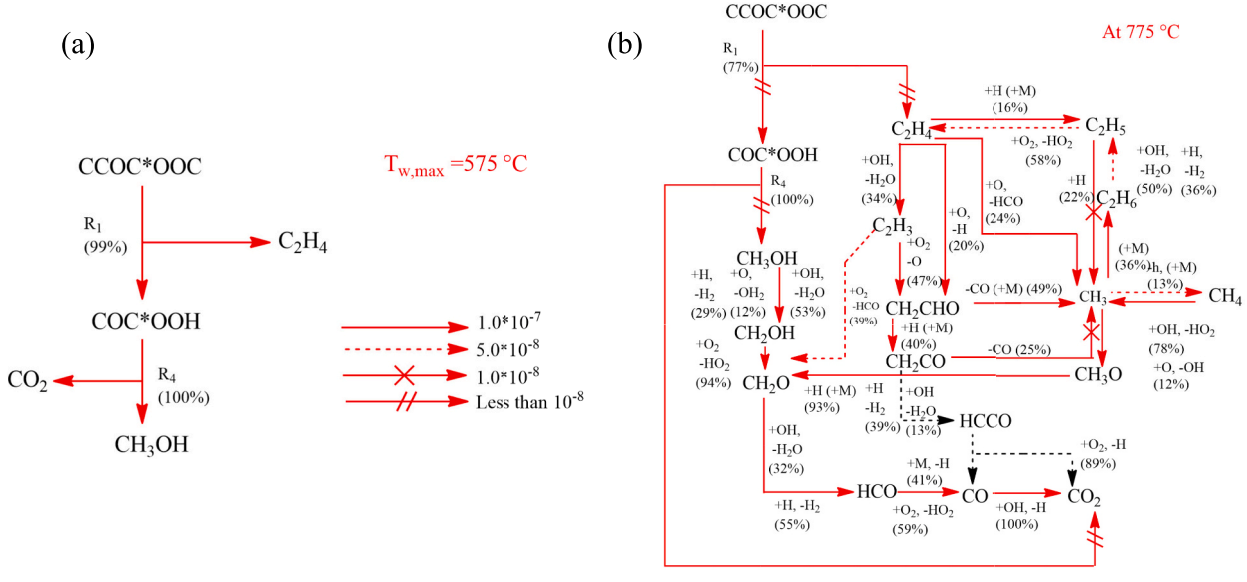

Fig. 22. Pathways for the oxidation of EMC in MFR at 1.0 atm, $T_{w,max}$ = 576 °C and 776 °C [76].

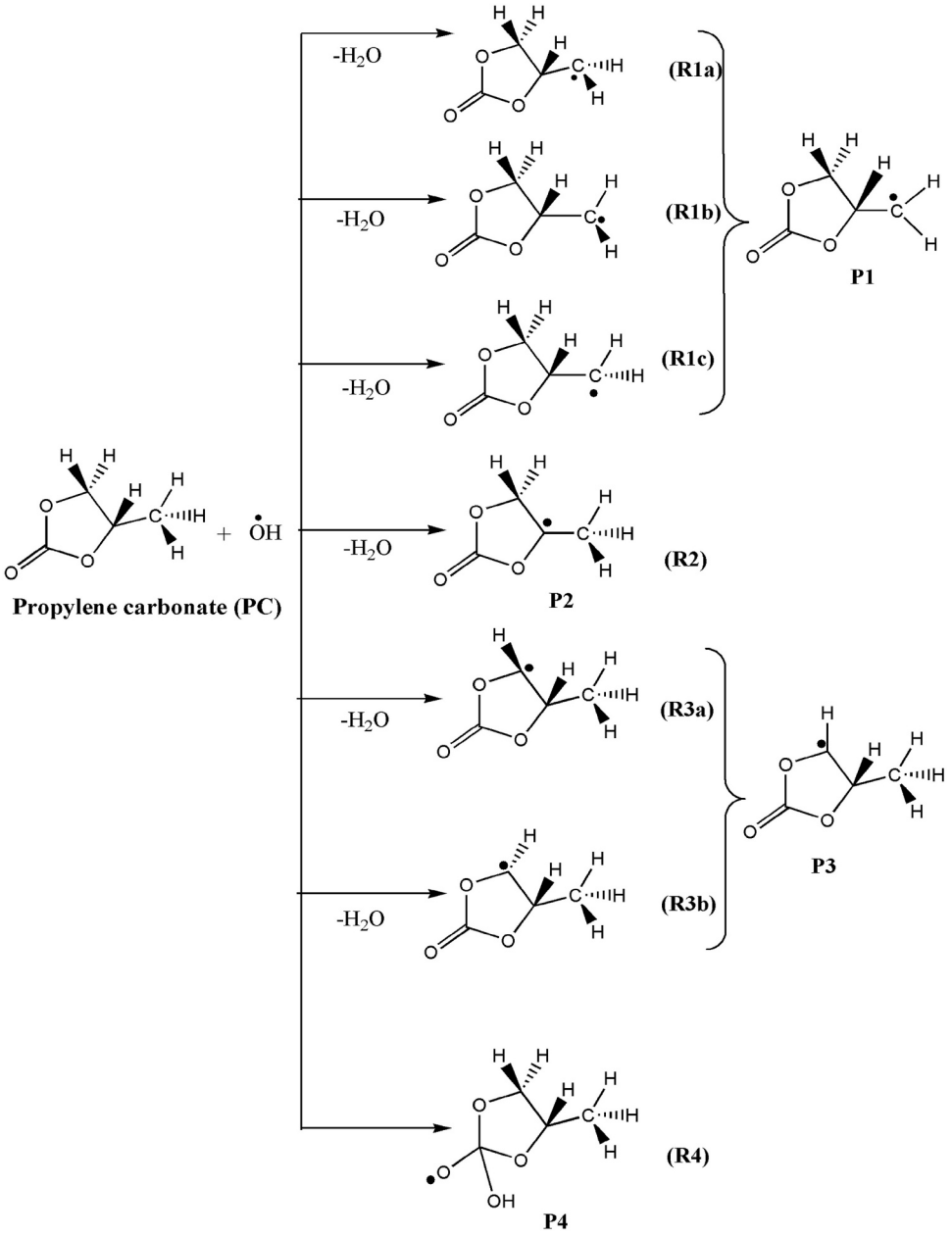

Fig. 23. Reaction pathway of PC [111].

involves the complex reaction between cathode and electrolyte. Although electrolytes exhibit little reactivity with ground-state O_2 at low temperatures, they can be oxidized by some potential active oxidizers such as cathode metal oxides and singlet O_2 at low temperatures. These reactions can lead to gas generation, progressive exothermal reactivity and increase internal pressure, all of which may ultimate full scale thermal runaway.

This review is mainly focused on chemical kinetics of electrolytes at various temperatures and pressure, from which we suspect the low temperature thermal runaway is due to the electrolyte-electrode interfacial reactions above. Unfortunately, the relevant heterogeneous kinetic mechanisms are very lacking and deserve comprehensive future studies. The potential research direction for the in-depth study on the low temperature thermal runaway is recommended here: 1) The chemical kinetics of electrolyte and cathode materials can be investigated using a flow reactor coupled with gas chromatography (GC) under the conditions of long residence time, atmospheric pressure and low temperature. 2) The theoretical computation of surface reactions between electrolyte and cathode materials by using DFT computation for the kinetic mechanism and studying their low temperature oxidation in the electrolysis process. Moreover, carbonates-based electrolytes have shown reactivity at low temperatures when interacting with cathode materials, and similar species have been observed during thermal runaways events [126]. Electrochemistry side reaction is based on cell design and using DEMS cells to investigate the product species during charging and discharging of cells. The electrochemistry side reaction will be considered in future study.

6. Conclusion and future directions

The advancement and adoption of lithium-ion batteries (LIBs) have greatly improved convenience across various aspects of our daily lives. However, safety is an ongoing concern that necessitates immediate investigation, particularly concerning lithium-ion batteries (LIBs) with

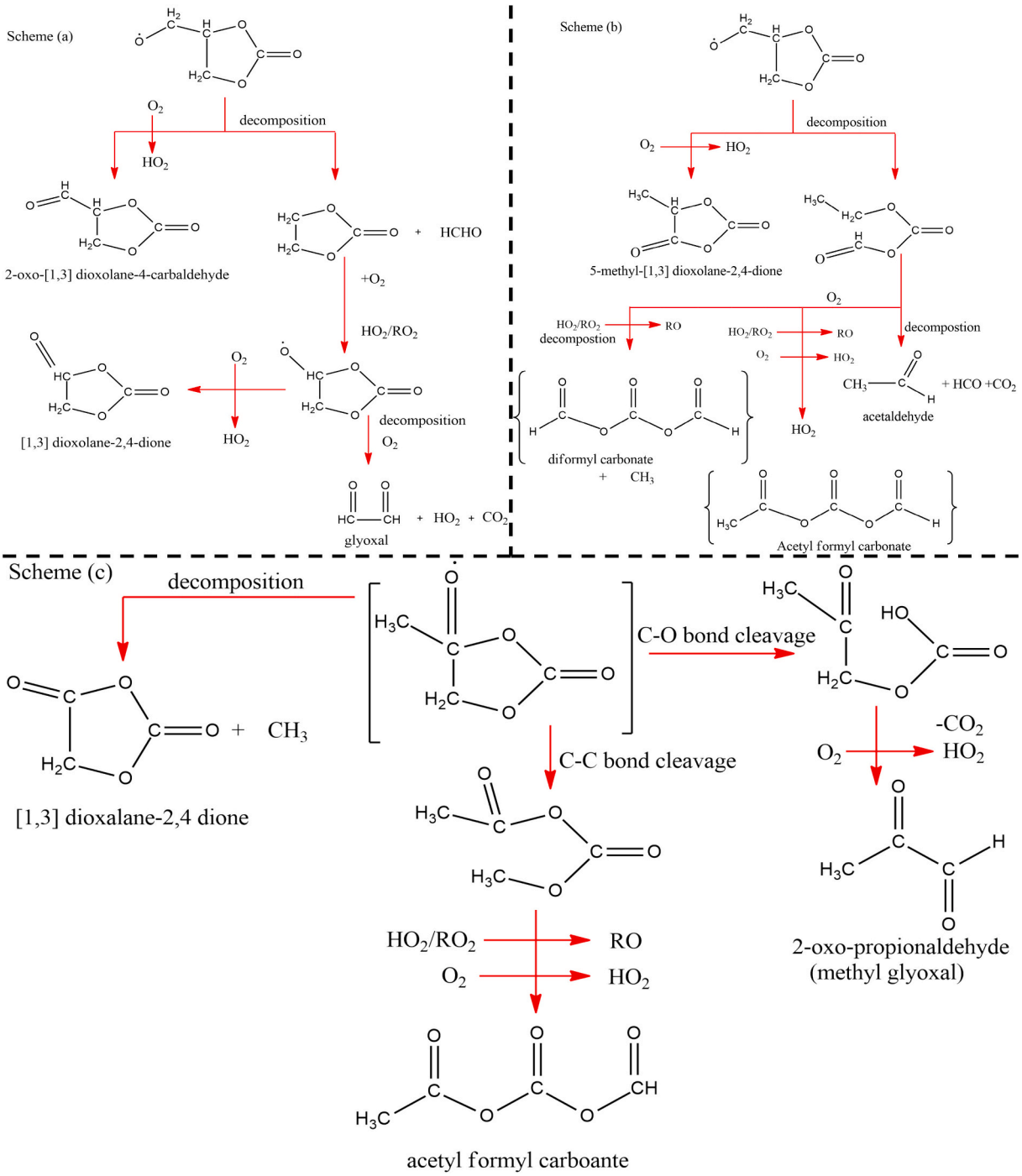

Fig. 24. Possible reaction path of propylene carbonate [112].

high energy density. This review examines the chemical kinetics of carbonate-based electrolytes of lithium-ion batteries. The study involves three phases. In the first phase, the gas-phase reactivity of various carbonate solvents (e.g., DEC, VC, DMC, FEC, EMC, PC, EC) in lithium-ion batteries was investigated using multiple reactors equipped with GC and MBSM for product detection. Resulting products like CO, CO_2, CH_4, etc., were observed under different conditions and verified through experiments and kinetic modeling. The coexistence of CO_2 and CO within the battery and decomposition patterns with temperature and state of charge were noted [127]. In second phase, gas-phase chemical kinetic modeling of various carbonate solvents (e.g., DEC, VC, DMC, FEC, EMC, PC, EC) for lithium-ion batteries has been developed to analyses the reaction mechanism. It has been proven that resulting products, such as CO, CO_2, CH_4, CH_3CHO, CH_2O, C_2H_5OH, C_2H_4 etc., were observed under different temperature and pressure conditions, which have been verified through experiments. The gases evolved during the oxidation of the electrolyte exhibited similar species as those observed during thermal runaway events. This research primarily examines the heterogeneous reactions between carbonate-based liquid electrolytes and cathode materials, particularly under regulated low-temperature circumstances utilizing reactors such as flow reactors, shock tubes, and rapid compression machines. The aim is to replicate real-time thermal conditions pertinent to liquid electrolytes and analyze their combustion characteristics at initial temperatures (150–250 °C). For liquid

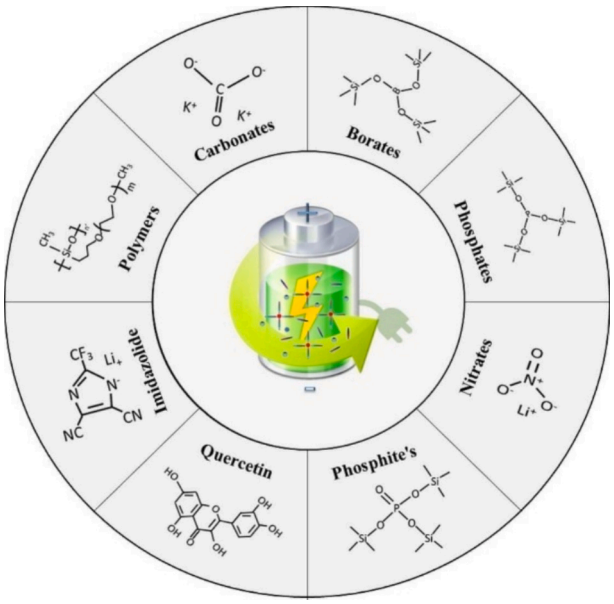

Fig. 25. Various additives for lithium-ion battery applications [118]. Copyright © 2023, Reproduced from Elsevier.

electrolyte, additives can enhance the fire safety concern. This new type of experiment is more helpful for selecting additives and compatible with cathodes. Although recent developments in solid-state electrolytes and their thermal stability are significant, they are beyond the intended focus of this study.

First challenge:

Studies have shown that most carbonate-based electrolytes exhibit stability at temperatures below 380–400 °C. However, it has been observed that batteries may experience failure when operating at lower temperatures, specifically between 125 and 200 °C.

Future direction:

Designing a new type of reactor such as flow reactor (FR), continuous stirred-tank reactor (CSTR), jet stirrer reactor (JSR) and constant volume combustion bomb (CVCB) for investigating carbonate-based electrolytes in lithium-ion batteries would enable us to make significant scientific contributions in this field.

- An automated temperature and pressure-controlled reactor should be designed using fused silica (quartz materials) for real time combustion of carbonate-based electrolytes using high speed camera and should be coupled with Micro-GC and molecular beam and mass spectrometry (MBMS) for analyzing the product species.
- To develop the realistic representation of battery environment in the reactors, enabling reliable and accurate operating conditions.
- Investigating the low temperature chemistry of different carbonate-based electrolytes at low pressure (1 atm), providing valuable insight into chemistry of various electrolytes that can contribute to the fire safety of lithium-ion batteries.

Second challenge:

Currently, there is no comprehensive kinetic model of DMC, DEC, EMC, and EC based electrolytes of lithium-ion batteries at low temperature range 125–350 °C and low pressure (1 atm) for understanding chemical kinetics of these electrolytes for fire safety perspective.

Future direction:

- Leveraging the previous kinetic model of different carbonate-based electrolytes, the new experimental data point and simulation results can be developed under various conditions as long residence time for reaction, low temperature (125–350 °C) and low pressure (1 atm).

Third challenge:

There is currently no study on heterogeneous reaction between carbonate-based electrolytes and cathode or anode materials of lithium-ion batteries, which are essential for analyzing the real scenario of reaction mechanism that leads to thermal runaway.

Future direction:

There are few possibilities to solve this challenge,

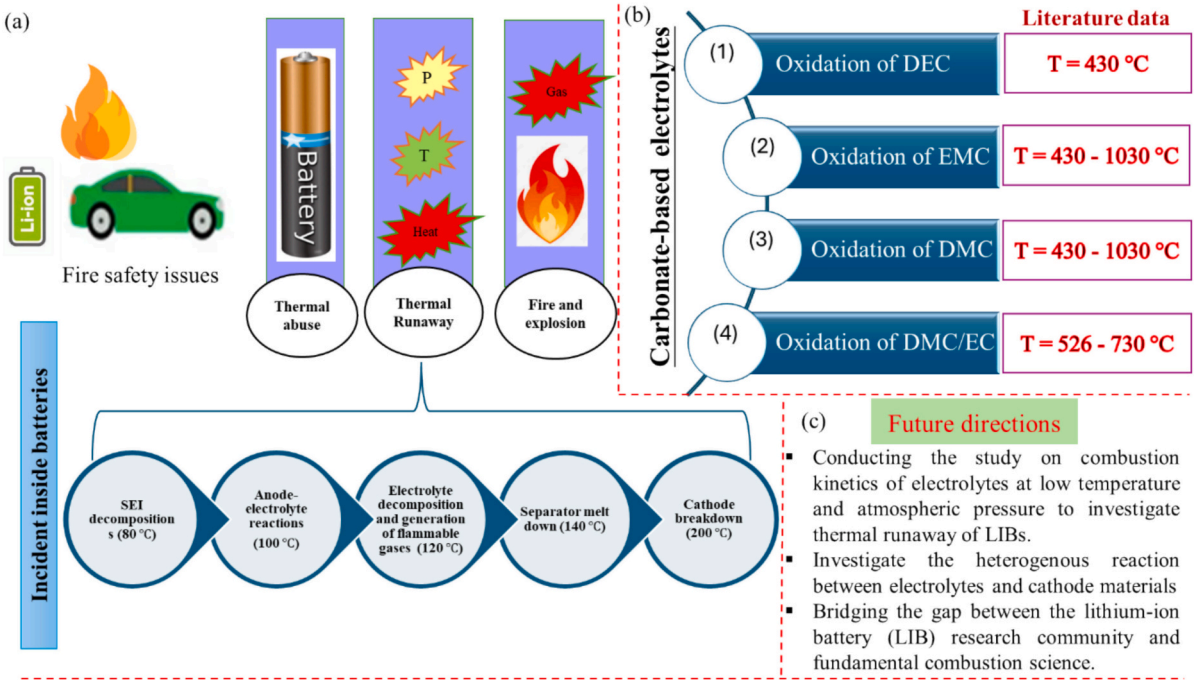

Fig. 26. Thermal runaway of lithium-ion batteries and oxidation mechanism of carbonate-based electrolytes.

- The oxidation of carbonate-based electrolytes can be carried out with ozone (O_3), as O_3 is decomposed into O_2 and singlet oxygen (O) state in different reactors. This process mimics cathode oxygen where the suitable environment for reaction under low temperature (125–350 °C) and low pressure (1 atm).
- Cathode materials should be placed in the reactor with continuous flow of vaporized carbonate-based electrolytes interacting with them. After heat treatment, cathode materials should be characterized by using different techniques such as XPS, SEM, XRD, Raman to access their chemical and thermal stability. The occurrence of thermal runaways in lithium-ion batteries is attributed to heterogeneous reactions taking place between the electrolyte and the electrode. To analyze the product species, it is recommended to develop a reactor integrated with gas chromatography (GC) and molecular beam and mass spectrometry (MBMS). This study assumes a significant role in examining the reactions between the carbonate-based electrolytes and the cathode, as well as detecting the various species involved.
- Density functional theory (DFT) studies are particularly helpful for understanding the heterogeneous reaction of electrolyte and cathode materials, supporting analysis of thermal runaway behavior.

CRediT authorship contribution statement

Ghulam Abbas Gohar: Project administration, Formal analysis, Data curation, Conceptualization, Writing – review & editing, Writing – original draft. **Liang An:** Supervision, Resources, Formal analysis, Writing – review & editing, Writing – original draft. **Hafiz Muhammad Ali:** Resources, Formal analysis, Writing – review & editing, Writing – original draft. **Hao Zhao:** Supervision, Project administration, Funding acquisition, Formal analysis, Conceptualization, Writing – review & editing, Writing – original draft.

Declaration of competing interest

The authors have declared that they have no conflicts of interest. There are no financial conflicts of interest to disclose because all authors have reviewed and approved the paper. We confirm that the contribution is unique, and it is not being considered for publication anywhere.

Acknowledgements

This work was financially supported by National Key R&D Program of China grant (2022YFB2502100).

Data availability

No data was used for the research described in the article.

References

[1] AIEA, Global EV outlook 2022: securing supplies for an electric future [Online]. Available: https://www.iea.org/reports/global-ev-outlook-2022, 2022.
[2] AFatih Birol, World Energy Outlook 2024, International Energy Agency, 2024 [Online]. Available: https://www.iea.org/reports/world-energy-outlook-2024.
[3] X. Wu, K. Song, X. Zhang, N. Hu, L. Li, W. Li, L. Zhang, H. Zhang, Safety issues in lithium ion batteries: materials and cell design, Frontiers in Energy Research 7 (2019) 65, https://doi.org/10.3389/fenrg.2019.00065.
[4] S.M. Abu, M. Hannan, M.H. Lipu, M. Mannan, P.J. Ker, M. Hossain, T.I. Mahlia, State of the art of lithium-ion battery material potentials: an analytical evaluations, issues and future research directions, J. Clean. Prod. (2023) 136246, https://doi.org/10.1016/j.jclepro.2023.136246.
[5] M.S. Whittingham, Lithium batteries and cathode materials, Chem. Rev. 104 (10) (2004) 4271–4302, https://doi.org/10.1021/cr020731c.
[6] H.-J. Noh, S. Youn, C.S. Yoon, Y.-K. Sun, Comparison of the structural and electrochemical properties of layered Li $[Ni_xCo_yMn_z]O_2$ (x= 1/3, 0.5, 0.6, 0.7, 0.8 and 0.85) cathode material for lithium-ion batteries, J. Power Sources 233 (2013) 121–130, https://doi.org/10.1016/j.jpowsour.2013.01.063.
[7] T. Ould Ely, D. Kamzabek, D. Chakraborty, Batteries safety: recent progress and current challenges, Frontiers in Energy Research 7 (2019) 71, https://doi.org/10.3389/fenrg.2019.00071.
[8] J.A. Sanguesa, V. Torres-Sanz, P. Garrido, F.J. Martinez, J.M. Marquez-Barja, A review on electric vehicles: technologies and challenges, Smart Cities 4 (1) (2021) 372–404, https://doi.org/10.3390/smartcities4010022.
[9] V. Ruiz, A. Pfrang, A. Kriston, N. Omar, P. Van den Bossche, L. Boon-Brett, A review of international abuse testing standards and regulations for lithium ion batteries in electric and hybrid electric vehicles, Renew. Sustain. Energy Rev. 81 (2018) 1427–1452, https://doi.org/10.1016/j.rser.2017.05.195.
[10] A.W. Golubkov, R. Planteu, P. Krohn, B. Rasch, B. Brunnsteiner, A. Thaler, V. Hacker, Thermal runaway of large automotive Li-ion batteries, RSC Adv. 8 (70) (2018) 40172–40186, https://doi.org/10.1039/C8RA06458J.
[11] X. Feng, D. Ren, X. He, M. Ouyang, Mitigating thermal runaway of lithium-ion batteries, Joule 4 (4) (2020) 743–770, https://doi.org/10.1016/j.joule.2020.02.010.
[12] D. Ouyang, M. Chen, Q. Huang, J. Weng, Z. Wang, J. Wang, A review on the thermal hazards of the lithium-ion battery and the corresponding countermeasures, Appl. Sci. 9 (12) (2019) 2483, https://doi.org/10.3390/app9122483.
[13] L. Kong, C. Li, J. Jiang, M.G. Pecht, Li-ion battery fire hazards and safety strategies, Energies 11 (9) (2018) 2191, https://doi.org/10.3390/en11092191.
[14] X. Han, L. Lu, Y. Zheng, X. Feng, Z. Li, J. Li, M. Ouyang, A review on the key issues of the lithium ion battery degradation among the whole life cycle, ETransportation 1 (2019) 100005, https://doi.org/10.1016/j.etran.2019.100005.
[15] S. Awasthi, A review on the optimization of electrolytes to enhance lithium-ion batteries' safety and performance under abuse conditions, Journal of Energy Storage 100 (2024) 113439, https://doi.org/10.1016/j.est.2024.113439.
[16] T. Zheng, M. Muneeswara, H. Bao, J. Huang, L. Zhang, D.S. Hall, S.T. Boles, W. Jin, Gas evolution in Li-ion rechargeable batteries: a review on operando sensing technologies, gassing mechanisms, and emerging trends, ChemElectroChem 11 (15) (2024) e202400065, https://doi.org/10.1002/celc.202400065.
[17] P.V. Chombo, Y. Laoonual, A review of safety strategies of a Li-ion battery, J. Power Sources 478 (2020) 228649, https://doi.org/10.1016/j.jpowsour.2020.228649.
[18] L. Song, Y. Zheng, Z. Xiao, C. Wang, T. Long, Review on thermal runaway of lithium-ion batteries for electric vehicles, J. Electron. Mater. 51 (1) (2022) 30–46, https://doi.org/10.1007/s11664-021-09281-0.
[19] R.D. McKerracher, J. Guzman-Guemez, R.G. Wills, S.M. Sharkh, D. Kramer, Advances in prevention of thermal runaway in lithium-ion batteries, Advanced Energy and Sustainability Research 2 (5) (2021) 2000059, https://doi.org/10.1002/aesr.202000059.
[20] N. Galushkin, N. Yazvinskaya, D. Galushkin, Mechanism of thermal runaway in lithium-ion cells, J. Electrochem. Soc. 165 (7) (2018) A1303, https://doi.org/10.1149/2.0611807jes.
[21] X. Feng, M. Ouyang, X. Liu, L. Lu, Y. Xia, X. He, Thermal runaway mechanism of lithium ion battery for electric vehicles: a review, Energy Storage Materials 10 (2018) 246–267, https://doi.org/10.1016/j.ensm.2017.05.013.
[22] J. Wen, Y. Yu, C. Chen, A review on lithium-ion batteries safety issues: existing problems and possible solutions, Mater. Express 2 (3) (2012) 197–212, https://doi.org/10.1166/mex.2012.1075.
[23] Q. Wang, P. Ping, X. Zhao, G. Chu, J. Sun, C. Chen, Thermal runaway caused fire and explosion of lithium ion battery, J. Power Sources 208 (2012) 210–224, https://doi.org/10.1016/j.jpowsour.2012.02.038.
[24] X. Fu, G. Wang, D. Dang, Q. Liu, X. Xiong, C. Wu, Sulfuryl chloride as a functional additive towards dendrite-free and long-life Li metal anodes, J. Mater. Chem. A 7 (43) (2019) 25003–25009, https://doi.org/10.1039/C9TA09068A.
[25] X. Fu, X. Deng, Y. Deng, X. Xiong, Y. Zheng, Z. Zhang, D. Dang, G. Wang, Lithium perchlorate additive for dendritic-free and long-life Li metal batteries, Energy Fuel 36 (18) (2022) 11219–11226, https://doi.org/10.1021/acs.energyfuels.2c02242.
[26] J. Lu, X. Fu, K. Shi, Y. Xu, D. Dang, Y. Min, Q. Liu, Y. Zheng, In situ construction of a LiF/LiCl-rich solid electrolyte interphase for lithium ion unimpeded transport, Ind. Eng. Chem. Res. 63 (14) (2024) 6249–6256, https://doi.org/10.1021/acs.iecr.3c04375.
[27] J. Lu, Q. Liu, Y. Zheng, K. Shi, D. Dang, Chain-segment ferry engineering from anchoring anion of the composite solid electrolyte enables fast lithium ion transport, Chem. Eng. Sci. 303 (2025) 120962, https://doi.org/10.1016/j.ces.2024.120962.
[28] A. Bonakdarpour, I. Stoševski, A. Tiwari, S.R. Smith, B. Way, D.P. Wilkinson, Impact of electrolyte volume on the cycling performance and impedance growth of 18650 Li-ion cells, J. Electrochem. Soc. 171 (2) (2024) 020543, https://doi.org/10.1149/1945-7111/ad27b6.
[29] S.J. An, J. Li, C. Daniel, H.M. Meyer III, S.E. Trask, B.J. Polzin, D.L. Wood III, Electrolyte volume effects on electrochemical performance and solid electrolyte interphase in Si-graphite/NMC lithium-ion pouch cells, ACS Appl. Mater. Interfaces 9 (22) (2017) 18799–18808, https://doi.org/10.1021/acsami.7b03617.
[30] B. Dong, L. Wang, L. Hu, J. Fang, Z. Wang, Exploring the oxidation chemistry of diethyl carbonate in lithium-ion battery thermal runaway using SVUV-PIMS, Proc. Combust. Inst. 40 (1–4) (2024) 105479, https://doi.org/10.1016/j.proci.2024.105479.
[31] Y. Li, X. Liu, L. Wang, X. Feng, D. Ren, Y. Wu, G. Xu, L. Lu, J. Hou, W. Zhang, Thermal runaway mechanism of lithium-ion battery with $LiNi_{0.8}Mn_{0.1}Co_{0.1}O_2$ cathode materials, Nano Energy 85 (2021) 105878, https://doi.org/10.1016/j.nanoen.2021.105878.

[32] H. Zhang, H. Liu, L.F. Piper, M.S. Whittingham, G. Zhou, Oxygen loss in layered oxide cathodes for Li-ion batteries: mechanisms, effects, and mitigation, Chem. Rev. 122 (6) (2022) 5641–5681, https://doi.org/10.1021/acs.chemrev.1c00327.

[33] A. Manthiram, X. Yu, S. Wang, Lithium battery chemistries enabled by solid-state electrolytes, Nature Reviews Materials 2 (4) (2017) 1–16, https://doi.org/10.1038/natrevmats.2016.103.

[34] Q. Zhao, S. Stalin, C.-Z. Zhao, L.A. Archer, Designing solid-state electrolytes for safe, energy-dense batteries, Nat. Rev. Mater. 5 (3) (2020) 229–252, https://doi.org/10.1038/s41578-019-0165-5.

[35] K. Matsumoto, K. Inoue, K. Utsugi, A highly safe battery with a non-flammable triethyl-phosphate-based electrolyte, J. Power Sources 273 (2015) 954–958, https://doi.org/10.1016/j.jpowsour.2014.09.086.

[36] Q. Zheng, Y. Yamada, R. Shang, S. Ko, Y.-Y. Lee, K. Kim, E. Nakamura, A. Yamada, A cyclic phosphate-based battery electrolyte for high voltage and safe operation, Nat. Energy 5 (4) (2020) 291–298, https://doi.org/10.1038/s41560-020-0567-z.

[37] Z. Zeng, V. Murugesan, K.S. Han, X. Jiang, Y. Cao, L. Xiao, X. Ai, H. Yang, J.-G. Zhang, M.L. Sushko, Non-flammable electrolytes with high salt-to-solvent ratios for Li-ion and Li-metal batteries, Nat. Energy 3 (8) (2018) 674–681, https://doi.org/10.1038/s41560-018-0196-y.

[38] P. Shi, H. Zheng, X. Liang, Y. Sun, S. Cheng, C. Chen, H. Xiang, A highly concentrated phosphate-based electrolyte for high-safety rechargeable lithium batteries, Chem. Commun. 54 (35) (2018) 4453–4456, https://doi.org/10.1039/C8CC00994E.

[39] J. Wang, Y. Yamada, K. Sodeyama, E. Watanabe, K. Takada, Y. Tateyama, A. Yamada, Fire-extinguishing organic electrolytes for safe batteries, Nat. Energy 3 (1) (2018) 22–29, https://doi.org/10.1038/s41560-017-0033-8.

[40] R. Kido, T. Horikawa, A. Sano, T. Nagashima, R. Okada, M. Inaba, T. Doi, Highly safe quasi-solid-state lithium ion batteries with two kinds of nearly saturated and non-flammable electrolyte solutions, Journal of Energy Storage 102 (2024) 114115, https://doi.org/10.1016/j.est.2024.114115.

[41] E. Hu, Y. Chen, Z. Zhang, L. Pan, Q. Li, Y. Cheng, Z. Huang, Experimental and kinetic study on ignition delay times of dimethyl carbonate at high temperature, Fuel 140 (2015) 626–632, https://doi.org/10.1016/j.fuel.2014.10.013.

[42] T. Atherley, S. de Persis, N. Chaumeix, Y. Fernandes, A. Bry, A. Comandini, O. Mathieu, S. Alturaifi, C. Mulvihill, E. Petersen, Laminar flame speed and shock-tube multi-species laser absorption measurements of dimethyl carbonate oxidation and pyrolysis near 1 atm, Proc. Combust. Inst. 38 (1) (2021) 977–985, https://doi.org/10.1016/j.proci.2020.06.333.

[43] W. Sun, B. Yang, N. Hansen, C.K. Westbrook, F. Zhang, G. Wang, K. Moshammer, C.K. Law, An experimental and kinetic modeling study on dimethyl carbonate (DMC) pyrolysis and combustion, Combust. Flame 164 (2016) 224–238, https://doi.org/10.1016/j.combustflame.2015.11.019.

[44] A. Sinha, M. Thomson, The chemical structures of opposed flow diffusion flames of C3 oxygenated hydrocarbons (isopropanol, dimethoxy methane, and dimethyl carbonate) and their mixtures, Combust. Flame 136 (4) (2004) 548–556, https://doi.org/10.1016/j.combustflame.2003.12.011.

[45] K. Kanayama, S. Takahashi, S. Morikura, H. Nakamura, T. Tezuka, K. Maruta, Study on oxidation and pyrolysis of carbonate esters using a micro flow reactor with a controlled temperature profile. Part I: reactivities of dimethyl carbonate, ethyl methyl carbonate and diethyl carbonate, Combust. Flame 237 (2022) 111810, https://doi.org/10.1016/j.combustflame.2021.111810.

[46] M. Henriksen, K. Vaagseather, A.V. Gaathaug, J. Lundberg, S. Forseth, D. Bjerketvedt, Laminar burning velocity of the dimethyl carbonate–air mixture formed by the Li-ion electrolyte solvent, Combust. Explos. Shock Waves 56 (4) (2020) 383–393, https://doi.org/10.1134/S0010508220040024.

[47] M.U. Alzueta, P. Salinas, Á. Millera, R. Bilbao, M. Abián, A study of dimethyl carbonate conversion and its impact to minimize soot and NO emissions, Proc. Combust. Inst. 36 (3) (2017) 3985–3993, https://doi.org/10.1016/j.proci.2016.07.086.

[48] K. Alexandrino, M.U. Alzueta, H.J. Curran, An experimental and modeling study of the ignition of dimethyl carbonate in shock tubes and rapid compression machine, Combust. Flame 188 (2018) 212–226, https://doi.org/10.1016/j.combustflame.2017.10.001.

[49] R. Yu, J. Liu, Y. Wu, C. Tang, W. Liang, H. Wang, M. Ouyang, Experimental and modeling study of the ignition kinetics of dimethyl carbonate, Combust. Flame 246 (2022) 112465, https://doi.org/10.1016/j.combustflame.2022.112465.

[50] R. Shahla, C. Togbé, S. Thion, R. Timothée, M. Lailliau, F. Halter, C. Chauveau, G. Dayma, P. Dagaut, Burning velocities and jet-stirred reactor oxidation of diethyl carbonate, Proc. Combust. Inst. 36 (1) (2017) 553–560, https://doi.org/10.1016/j.proci.2016.06.041.

[51] H. Nakamura, H.J. Curran, A.P. Córdoba, W.J. Pitz, P. Dagaut, C. Togbé, S. M. Sarathy, M. Mehl, J.R. Agudelo, F. Bustamante, An experimental and modeling study of diethyl carbonate oxidation, Combust. Flame 162 (4) (2015) 1395–1405, https://doi.org/10.1016/j.combustflame.2014.11.002.

[52] J. Zhang, A. Zhong, Z. Huang, D. Han, Experimental and kinetic study on the stabilities and gas generation of typical electrolyte solvent components under oxygen-lean oxidation and pyrolysis conditions, SCIENCE CHINA Technol. Sci. 65 (12) (2022) 2883–2894, https://doi.org/10.1007/s11431-022-2184-x.

[53] W. Sun, C. Huang, T. Tao, F. Zhang, W. Li, N. Hansen, B. Yang, Exploring the high-temperature kinetics of diethyl carbonate (DEC) under pyrolysis and flame conditions, Combust. Flame 181 (2017) 71–81, https://doi.org/10.1016/j.combustflame.2017.03.009.

[54] H. Zhao, S. Liu, C. Yan, C. Huang, Y. Qi, F. Zhang, Y. Ju, Studies of ozone-sensitized low-and high-temperature oxidations of diethyl carbonate, Chem. A Eur. J. 125 (8) (2021) 1760–1765, https://doi.org/10.1021/acs.jpca.0c09002.

[55] S.P. Cooper, C.M. Grégoire, Y.M. Almarzooq, E.L. Petersen, O. Mathieu, Experimental kinetics study on diethyl carbonate oxidation, Fuels 4 (2) (2023) 243–260, https://doi.org/10.3390/fuels4020015.

[56] K. Kanayama, S. Takahashi, H. Nakamura, T. Tezuka, K. Maruta, Experimental and modeling study on pyrolysis of ethylene carbonate/dimethyl carbonate mixture, Combust. Flame 245 (2022) 112359, https://doi.org/10.1016/j.combustflame.2022.112359.

[57] P. Sela, Y. Zhang, J. Herzler, M. Fikri, C. Schulz, S. Peukert, Pyrolysis of diethyl carbonate: shock-tube and flow-reactor measurements and modeling, Proc. Combust. Inst. 38 (1) (2021) 987–996, https://doi.org/10.1016/j.proci.2020.07.052.

[58] C.M. Grégoire, S.P. Cooper, M. Khan-Ghauri, S.A. Alturaifi, E.L. Petersen, O. Mathieu, Pyrolysis study of dimethyl carbonate, diethyl carbonate, and ethyl methyl carbonate using shock-tube spectroscopic CO measurements and chemical kinetics investigation, Combust. Flame 249 (2023) 112594, https://doi.org/10.1016/j.combustflame.2022.112594.

[59] R. Yu, J. Liu, Y. Wu, C. Tang, Experimental and modeling study on ignition kinetics of ethyl methyl carbonate, Combust. Flame 261 (2024) 113318, https://doi.org/10.1016/j.combustflame.2024.113318.

[60] Q. Luo, L. Zheng, J. Wang, X. Shao, X. Wang, H. Li, C. Niu, Z. Peng, Flame propagation characteristics and reaction kinetics of electrolyte solvent vapor (ethylene carbonate) released from lithium-ion batteries, Appl. Therm. Eng. (2025) 125543, https://doi.org/10.1016/j.applthermaleng.2025.125543.

[61] Q. Luo, L. Zheng, J. Wang, H. Jia, X. Wang, S. Zhang, D. Wang, J. Lu, Investigation of chemical kinetic models for electrolyte solvent vapors released from thermal runaway lithium-ion batteries, Journal of Energy Storage 107 (2025) 114932, https://doi.org/10.1016/j.est.2024.114932.

[62] X. Yang, W. Yang, C. Liu, M. Yu, Experimental and kinetic study on the explosion characteristics of lithium-ion battery vented gases, Journal of Energy Storage 98 (2024) 113101, https://doi.org/10.1016/j.est.2024.113101.

[63] J. Deng, W. Yang, Y. Zhang, L. Pan, F. Kang, X. Ji, H. Wu, Combustion characteristics and fire risk assessment of EC/DMC/EMC electrolytes for Li-ion batteries, Journal of Energy Storage 110 (2025) 115308, https://doi.org/10.1016/j.est.2025.115308.

[64] S. Peukert, R. Sivaramakrishnan, J. Michael, High temperature shock tube studies on the thermal decomposition of O_3 and the reaction of dimethyl carbonate with O-atoms, Chem. A Eur. J. 117 (18) (2013) 3729–3738, https://doi.org/10.1021/jp400613p.

[65] S. Peukert, R. Sivaramakrishnan, J. Michael, High temperature shock tube and theoretical studies on the thermal decomposition of dimethyl carbonate and its bimolecular reactions with H and D-atoms, Chem. A Eur. J. 117 (18) (2013) 3718–3728, https://doi.org/10.1021/jp312643k.

[66] M. AlAbbad, B.R. Giri, M. Szőri, B. Viskolcz, A. Farooq, A high temperature kinetic study for the thermal unimolecular decomposition of diethyl carbonate, Chem. Phys. Lett. 684 (2017) 390–396, https://doi.org/10.1016/j.cplett.2017.07.020.

[67] H. Zhao, X. Yang, Y. Ju, Kinetic studies of ozone assisted low temperature oxidation of dimethyl ether in a flow reactor using molecular-beam mass spectrometry, Combust. Flame 173 (2016) 187–194, https://doi.org/10.1016/j.combustflame.2016.08.008.

[68] C. Aiken, J. Self, R. Petibon, X. Xia, J. Paulsen, J. Dahn, A survey of in situ gas evolution during high voltage formation in Li-ion pouch cells, J. Electrochem. Soc. 162 (4) (2015) A760, https://doi.org/10.1149/2.0941504jes.

[69] R. Jung, M. Metzger, F. Maglia, C. Stinner, H.A. Gasteiger, Oxygen release and its effect on the cycling stability of $LiNi_xMn_yCo_zO_2$ (NMC) cathode materials for Li-ion batteries, J. Electrochem. Soc. 164 (7) (2017) A1361, https://doi.org/10.1149/2.0021707jes.

[70] S. Hess, M. Wohlfahrt-Mehrens, M. Wachtler, Flammability of Li-ion battery electrolytes: flash point and self-extinguishing time measurements, J. Electrochem. Soc. 162 (2) (2015) A3084, https://doi.org/10.1149/2.0121502jes.

[71] F. Guo, Y. Ozaki, K. Nishimura, N. Hashimoto, O. Fujita, Influence of lithium salts on the combustion characteristics of dimethyl carbonate-based electrolytes using a wick combustion method, Combust. Flame 213 (2020) 314–321, https://doi.org/10.1016/j.combustflame.2019.12.001.

[72] Y. Ren, Z. Huang, H. Miao, Y. Di, D. Jiang, K. Zeng, B. Liu, X. Wang, Combustion and emissions of a DI diesel engine fuelled with diesel-oxygenate blends, Fuel 87 (12) (2008) 2691–2697, https://doi.org/10.1016/j.fuel.2008.02.017.

[73] Q. Wang, B. Mao, S.I. Stoliarov, J. Sun, A review of lithium ion battery failure mechanisms and fire prevention strategies, Prog. Energy Combust. Sci. 73 (2019) 95–131, https://doi.org/10.1016/j.pecs.2019.03.002.

[74] A. Lecocq, G. Marlair, D. Tigreat, G.G. Eshetu, S. Laruelle, S. Grugeon, Safety-focused analysis of solvents used in electrolytes for large scale lithium-ion batteries, in: Batteries, 2013, https://doi.org/10.1039/C3CP51315G.

[75] S.J. Harris, A. Timmons, W.J. Pitz, A combustion chemistry analysis of carbonate solvents used in Li-ion batteries, J. Power Sources 193 (2) (2009) 855–858, https://doi.org/10.1016/j.jpowsour.2009.04.030.

[76] S. Takahashi, K. Kanayama, S. Morikura, H. Nakamura, T. Tezuka, K. Maruta, Study on oxidation and pyrolysis of carbonate esters using a micro flow reactor with a controlled temperature profile. Part II: chemical kinetic modeling of ethyl methyl carbonate, Combust. Flame 238 (2022) 111878, https://doi.org/10.1016/j.combustflame.2021.111878.

[77] J. Chan, A. Tsolakis, J. Herreros, K. Kallis, C. Hergueta, S. Sittichompoo, M. Bogarra, Combustion, gaseous emissions and PM characteristics of di-methyl carbonate (DMC)-gasoline blend on gasoline direct injection (GDI) engine, Fuel 263 (2020) 116742, https://doi.org/10.1016/j.fuel.2019.116742.

[78] G.G. Eshetu, S. Grugeon, S. Laruelle, S. Boyanov, A. Lecocq, J.-P. Bertrand, G. Marlair, In-depth safety-focused analysis of solvents used in electrolytes for large scale lithium ion batteries, Phys. Chem. Chem. Phys. 15 (23) (2013) 9145–9155, https://doi.org/10.1039/C3CP51315G.

[79] R. Spotnitz, J. Franklin, Abuse behavior of high-power, lithium-ion cells, J. Power Sources 113 (1) (2003) 81–100, https://doi.org/10.1016/S0378-7753(02)00488-3.

[80] A.W. Golubkov, D. Fuchs, J. Wagner, H. Wiltsche, C. Stangl, G. Fauler, G. Voitic, A. Thaler, V. Hacker, Thermal-runaway experiments on consumer Li-ion batteries with metal-oxide and olivin-type cathodes, RSC Adv. 4 (7) (2014) 3633–3642, https://doi.org/10.1039/C3RA45748F.

[81] L. Zhang, P. Zhao, M. Xu, X. Wang, Computational identification of the safety regime of Li-ion battery thermal runaway, Appl. Energy 261 (2020) 114440, https://doi.org/10.1016/j.apenergy.2019.114440.

[82] P. Ribière, S. Grugeon, M. Morcrette, S. Boyanov, S. Laruelle, G. Marlair, Investigation on the fire-induced hazards of Li-ion battery cells by fire calorimetry, Energ. Environ. Sci. 5 (1) (2012) 5271–5280, https://doi.org/10.1039/C1EE02218K.

[83] G.G. Eshetu, J.-P. Bertrand, A. Lecocq, S. Grugeon, S. Laruelle, M. Armand, G. Marlair, Fire behavior of carbonates-based electrolytes used in Li-ion rechargeable batteries with a focus on the role of the LiPF+ and LiFSI salts, J. Power Sources 269 (2014) 804–811, https://doi.org/10.1016/j.jpowsour.2014.07.065.

[84] G.G. Eshetu, J.-P. Bertrand, A. Lecocq, S. Grugeon, S. Laruelle, M. Armand, G. Marlair, Fire behavior of carbonates-based electrolytes used in Li-ion rechargeable batteries with a focus on the role of the LiPF6 and LiFSI salts, J. Power Sources 269 (2014) 804–811, https://doi.org/10.1016/j.jpowsour.2014.07.065.

[85] T.R. Jow, K. Xu, O. Borodin, M. Ue, Electrolytes for Lithium and Lithium-Ion Batteries, Springer, 2014.

[86] W. Zhang, X. Chen, Q. Chen, C. Ding, J. Liu, M. Chen, J. Wang, Combustion calorimetry of carbonate electrolytes used in lithium ion batteries, J. Fire Sci. 33 (1) (2015) 22–36, https://doi.org/10.1177/0734904114550789.

[87] Q. Huang, J. Weng, D. Ouyang, M. Chen, X. Wang, J. Wang, Comparative studies on the combustion characteristics of electrolytes and carbonate mixed solvents with flame retardant additives under low pressures, Case Studies in Thermal Engineering 43 (2023) 102810, https://doi.org/10.1016/j.csite.2023.102810.

[88] M. Intellegent, Lithium-ion battery's electrolyte solvent markeet - growth, trends, covid-19 impact, and forecasts (2023–2028). https://shorturl.at/DRSY0 (accessed 20 May, 2023).

[89] M. Parhizi, L.E. Caceres-Martinez, B.A. Modereger, H.I. Kenttämaa, G. Kilaz, J. K. Ostanek, Determining the composition of carbonate solvent systems used in lithium-ion batteries without salt removal, Energies 15 (8) (2022) 2805, https://doi.org/10.3390/en15082805.

[90] Y. Fu, S. Lu, L. Shi, X. Cheng, H. Zhang, Combustion characteristics of electrolyte pool fires for lithium ion batteries, J. Electrochem. Soc. 163 (9) (2016) A2022, https://doi.org/10.1149/2.0721609jes.

[91] P. Sun, R. Bisschop, H. Niu, X. Huang, A review of battery fires in electric vehicles, Fire Technol. 56 (4) (2020) 1361–1410, https://doi.org/10.1007/s10694-020-00958-2.

[92] R. Bisschop, O. Willstrand, F. Amon, M. Rosenggren, Fire Safety of Lithium-Ion Batteries in Road Vehicles, RISE Research Institutes of Sweden, 2019, https://doi.org/10.13140/RG.2.2.18738.15049.

[93] M. Muratori, M. Alexander, D. Arent, M. Bazilian, P. Cazzola, E.M. Dede, J. Farrell, C. Gearhart, D. Greene, A. Jenn, The rise of electric vehicles—2020 status and future expectations, Progress in Energy 3 (2) (2021) 022002, https://doi.org/10.1088/2516-1083/abe0ad.

[94] Y. Fernandes, A. Bry, S. De Persis, Identification and quantification of gases emitted during abuse tests by overcharge of a commercial Li-ion battery, J. Power Sources 389 (2018) 106–119, https://doi.org/10.1016/j.jpowsour.2018.03.034.

[95] C. Thomas Avedisian, W.-C. Kuo, W. Tsang, A. Lowery, High temperature thermal decomposition of diethyl carbonate by pool film boiling, J. Heat Transfer 140 (6) (2018), https://doi.org/10.1115/1.4038572.

[96] G.N. Rimondino, W.J. Peláez, F.E. Malanca, Atmospheric photo-oxidation of diethyl carbonate: kinetics, products, and reaction mechanism, Chem. A Eur. J. 124 (1) (2019) 56–62, https://doi.org/10.1021/acs.jpca.9b09887.

[97] M. Bilde, T. Møgelberg, J. Sehested, O. Nielsen, T. Wallington, M. Hurley, S. Japar, M. Dill, V. Orkin, T. Buckley, Atmospheric chemistry of dimethyl carbonate: reaction with OH radicals, UV spectra of CH_3OC (O) OCH_2 and CH_3OC (O) OCH_2O_2 radicals, reactions of CH_3OC (O) OCH_2O_2 with NO and NO_2, and fate of CH_3OC (O) OCH_2O radicals, Chem. A Eur. J. 101 (19) (1997) 3514–3525, https://doi.org/10.1021/jp961664r.

[98] A.S. Gordon, W.P. Norris, A study of the pyrolysis of methyl ethyl and diethyl carbonates in the gas phase, J. Phys. Chem. 69 (9) (1965) 3013–3017, https://doi.org/10.1021/j100893a032.

[99] D. Ortiz, V. Steinmetz, D. Durand, S. Legand, V. Dauvois, P. Maître, S. Le Caër, Radiolysis as a solution for accelerated ageing studies of electrolytes in Lithium-ion batteries, Nat. Commun. 6 (1) (2015) 1–8, https://doi.org/10.1038/ncomms7950.

[100] P.A. Glaude, W.J. Pitz, M.J. Thomson, Chemical kinetic modeling of dimethyl carbonate in an opposed-flow diffusion flame, Proc. Combust. Inst. 30 (1) (2005) 1111–1118, https://doi.org/10.1016/j.proci.2004.08.096.

[101] F. Khaled, B.R. Giri, M. Szőri, T.V.-T. Mai, L.K. Huynh, A. Farooq, A combined high-temperature experimental and theoretical kinetic study of the reaction of dimethyl carbonate with OH radicals, Phys. Chem. Chem. Phys. 19 (10) (2017) 7147–7157, https://doi.org/10.1039/C6CP07318B.

[102] M. Gnanaprakasam, L. Sandhiya, K. Senthilkumar, Mechanism and kinetics of the oxidation of dimethyl carbonate by hydroxyl radical in the atmosphere, Environ. Sci. Pollut. Res. 26 (4) (2019) 3357–3367, https://doi.org/10.1007/s11356-018-3831-z.

[103] Y. Ein-Eli, Dimethyl carbonate (DMC) electrolytes–the effect of solvent purity on Li–ion intercalation into graphite anodes, Electrochem. Commun. 4 (8) (2002) 644–648, https://doi.org/10.1016/S1388-2481(02)00407-1.

[104] D. Aurbach, Y. Talyosef, B. Markovsky, E. Markevich, E. Zinigrad, L. Asraf, J. S. Gnanaraj, H.-J. Kim, Design of electrolyte solutions for Li and Li-ion batteries: a review, Electrochim. Acta 50 (2–3) (2004) 247–254, https://doi.org/10.1016/j.electacta.2004.01.090.

[105] M.E. Bardin, E.V. Ivanov, E.J. Nilsson, V.A. Vinokurov, A.A. Konnov, Laminar burning velocities of dimethyl carbonate with air, Energy Fuel 27 (9) (2013) 5513–5517, https://doi.org/10.1021/ef401108a.

[106] S. Dooley, H.J. Curran, J.M. Simmie, Autoignition measurements and a validated kinetic model for the biodiesel surrogate, methyl butanoate, Combust. Flame 153 (1–2) (2008) 2–32, https://doi.org/10.1016/j.combustflame.2008.01.005.

[107] S. Dooley, M. Burke, M. Chaos, Y. Stein, F. Dryer, V.P. Zhukov, O. Finch, J. Simmie, H. Curran, Methyl formate oxidation: speciation data, laminar burning velocities, ignition delay times, and a validated chemical kinetic model, Int. J. Chem. Kinet. 42 (9) (2010) 527–549, https://doi.org/10.1002/kin.20512.

[108] K. Alexandrino, A. Millera, R. Bilbao, M.U. Alzueta, Experimental and simulation study of the high pressure oxidation of dimethyl carbonate, Fuel 309 (2022) 122154, https://doi.org/10.1016/j.fuel.2021.122154.

[109] S.-C. Kinoshita, M. Kotato, Y. Sakata, M. Ue, Y. Watanabe, H. Morimoto, S.-I. Tobishima, Effects of cyclic carbonates as additives to γ-butyrolactone electrolytes for rechargeable lithium cells, J. Power Sources 183 (2) (2008) 755–760, https://doi.org/10.1016/j.jpowsour.2008.05.035.

[110] K. Yasunaga, J. Simmie, H. Curran, T. Koike, O. Takahashi, Y. Kuraguchi, Y. Hidaka, Detailed chemical kinetic mechanisms of ethyl methyl, methyl tert-butyl and ethyl tert-butyl ethers: the importance of uni-molecular elimination reactions, Combust. Flame 158 (6) (2011) 1032–1036, https://doi.org/10.1016/j.combustflame.2010.10.012.

[111] S. Paul, J. Deka, A. Deka, N.K. Gour, Degradation mechanism of propylene carbonate initiated by hydroxyl radical and fate of its product radicals: a hybrid density functional study, Atmos. Environ. 216 (2019) 116952, https://doi.org/10.1016/j.atmosenv.2019.116952.

[112] I. Barnes, P. Wiesen, M. Gallus, Kinetics and mechanism of the OH-radical and Cl-atom oxidation of propylene carbonate, RSC Adv. 6 (100) (2016) 98234–98242, https://doi.org/10.1039/C6RA21952G.

[113] X. Sun, H. Lee, X.-Q. Yang, J. McBreen, Using a boron-based anion receptor additive to improve the thermal stability of LiPF6-based electrolyte for lithium batteries, Electrochem. Solid St. 5 (11) (2002) A248, https://doi.org/10.1149/1.1510321.

[114] X. Wang, E. Yasukawa, S. Kasuya, Nonflammable trimethyl phosphate solvent-containing electrolytes for lithium-ion batteries: I. Fundamental properties, J. Electrochem. Soc. 148 (10) (2001) A1058, https://doi.org/10.1149/1.1397773.

[115] P. Li, L. Chen, Z. Wen, D. Zhang, Y. Zhang, N. Zhang, G. Chen, X. Liu, Solvation chemistry of rare earth nitrates in carbonate electrolyte for advanced lithium metal batteries, Chem. Eng. J. 433 (2022) 134468, https://doi.org/10.1016/j.cej.2021.134468.

[116] M.-L. Lee, Y.-H. Li, J.-W. Yeh, H.C. Shih, Improvement in safety and cycle life of lithium-ion batteries by employing quercetin as an electrolyte additive, J. Power Sources 214 (2012) 251–257, https://doi.org/10.1016/j.jpowsour.2012.04.081.

[117] J.H. Won, H.S. Lee, L. Hamenu, M. Latifatu, Y.M. Lee, K.M. Kim, J. Oh, W.I. Cho, J.M. Ko, Improvement of low-temperature performance by adopting polydimethylsiloxane-g-polyacrylate and lithium-modified silica nanosalt as electrolyte additives in lithium-ion batteries, J. Ind. Eng. Chem. 37 (2016) 325–329, https://doi.org/10.1016/j.jpowsour.2012.04.081.

[118] R.I. Pushparaj, A.R. Kumar, G. Xu, Enhancing safety in lithium-ion batteries with additive-based liquid electrolytes: a critical review, Journal of Energy Storage 72 (2023) 108493, https://doi.org/10.1016/j.est.2023.108493.

[119] P.J. Bugryniec, E.G. Resendiz, S.M. Nwophoke, S. Khanna, C. James, S.F. Brown, Review of gas emissions from lithium-ion battery thermal runaway failure—considering toxic and flammable compounds, Journal of Energy Storage 87 (2024) 111288, https://doi.org/10.1016/j.est.2024.111288.

[120] C.-Y. Jhu, Y.-W. Wang, C.-M. Shu, J.-C. Chang, H.-C. Wu, Thermal explosion hazards on 18650 lithium ion batteries with a VSP2 adiabatic calorimeter, J. Hazard. Mater. 192 (1) (2011) 99–107, https://doi.org/10.1016/j.jhazmat.2011.04.097.

[121] J. Kahr, C. Groher, V. Schierer, E. Rosenberg, M. Jahn, Operando gas chromatography mass spectrometry for the continuous study of overcharge-induced electrolyte decomposition in lithium-ion batteries, J. Power Sources 615 (2024) 235038, https://doi.org/10.1016/j.jpowsour.2024.235038.

[122] N.P. Lebedeva, L. Boon-Brett, Considerations on the chemical toxicity of contemporary Li-ion battery electrolytes and their components, J. Electrochem. Soc. 163 (6) (2016) A821, https://doi.org/10.1149/2.0171606jes.

[123] J. Sun, J. Li, T. Zhou, K. Yang, S. Wei, N. Tang, N. Dang, H. Li, X. Qiu, L. Chen, Toxicity, a serious concern of thermal runaway from commercial Li-ion battery, Nano Energy 27 (2016) 313–319, https://doi.org/10.1016/j.nanoen.2016.06.031.

[124] A. Nedjalkov, J. Meyer, M. Köhring, A. Doering, M. Angelmahr, S. Dahle, A. Sander, A. Fischer, W. Schade, Toxic gas emissions from damaged lithium ion batteries—analysis and safety enhancement solution, Batteries 2 (1) (2016) 5, https://doi.org/10.3390/batteries2010005.

[125] H. Nozaki, H. Kondo, T. Shinohara, D. Setoyama, Y. Matsumoto, T. Sasaki, K. Isegawa, H. Hayashida, In situ neutron imaging of lithium-ion batteries during heating to thermal runaway, Sci. Rep. 13 (1) (2023) 22082, https://doi.org/10.1038/s41598-023-49399-1.

[126] G.A. Gohar, Chemical kinetics of electrolyte and cathode materials for enhancing fire safety in lithium-ion batteries. https://theses.lib.polyu.edu.hk/handle/200/13065, 2024.

[127] S.S. Zhang, Insight into the gassing problem of Li-ion battery, Frontiers in Energy Research 2 (2014) 59, https://doi.org/10.3389/fenrg.2014.00059.